

AEDC-TR-68-127

cy 7



## TWO-PHASE FLOW IN SPRAY COOLERS

H. A. Walls, J. P. Lamb, et al.  
The University of Texas at Austin  
Austin, Texas

June 1968

This document has been approved for public release  
and sale; its distribution is unlimited.



**ARNOLD ENGINEERING DEVELOPMENT CENTER  
AIR FORCE SYSTEMS COMMAND  
ARNOLD AIR FORCE STATION, TENNESSEE**

# *NOTICES*

When U. S. Government drawings specifications, or other data are used for any purpose other than a definitely related Government procurement operation, the Government thereby incurs no responsibility nor any obligation whatsoever, and the fact that the Government may have formulated, furnished, or in any way supplied the said drawings, specifications, or other data, is not to be regarded by implication or otherwise, or in any manner licensing the holder or any other person or corporation, or conveying any rights or permission to manufacture, use, or sell any patented invention that may in any way be related thereto.

Qualified users may obtain copies of this report from the Defense Documentation Center.

References to named commercial products in this report are not to be considered in any sense as an endorsement of the product by the United States Air Force or the Government.

TWO-PHASE FLOW  
IN SPRAY COOLERS

H. A. Walls, J. P. Lamb, et al.  
The University of Texas at Austin  
Austin, Texas

This document has been approved for public release  
and sale; its distribution is unlimited.

## FOREWORD

The research reported herein was performed at the Department of Mechanical Engineering, The University of Texas at Austin, for the Arnold Engineering Development Center (AEDC), Air Force Systems Command (AFSC), Arnold Air Force Station, Tennessee, under Contract AF40(600) - 1167, Program Element 6240518F, Project 5730, Task 04. The research was conducted between April 1, 1966, and August 31, 1967, and the manuscript of this report was submitted for publication on June 3, 1968.

The present research is the result of a number of contributions. Dr. Lamb and Dr. Walls served as principal investigators with Dr. J. T. Pogson assisting in the development of the two-phase theory. Mr. J. D. Lowther prepared the literature review in Section I. This will become a part of his doctoral dissertation on annular mist flows. Mr. E. F. Broome, another doctoral candidate, assisted in the development of the computer programs, while Mr. J. W. Jones performed the air flow experiments as a portion of his Master's thesis.

The reproducibles used in the reproduction of this report were supplied by the authors.

This technical report has been reviewed and is approved.

Eules L. Hively  
Research Division  
Directorate of Plans  
and Technology

Edward R. Feicht  
Colonel, USAF  
Director of Plans  
and Technology

**ABSTRACT**

The problem of estimating pressure drops with typical in-line bar, spray cooler configurations is discussed. Such coolers form an important component of facilities for rocket testing at simulated altitudes. In the present report, the complex nature of gas-liquid flows is first discussed. This is followed by a presentation of results of some simple experiments of air flow over a tube bank in a model spray-cooler section to determine the influence of this particular geometry on the drag coefficient. Based upon the information in these two sections, a semi-empirical analysis of two-phase flow in coolers is then developed and some results of the method are presented. Finally, recommendations are made concerning an experimental program which would enhance the further development of prediction techniques in cooler design.

## CONTENTS

	Page
ABSTRACT . . . . .	iii
NOMENCLATURE . . . . .	viii
I. GENERAL REMARKS . . . . .	1
1.1 Introduction . . . . .	1
1.2 Present State of Knowledge . . . . .	2
1.3 Flow Patterns . . . . .	3
1.4 Pressure Drop . . . . .	5
1.5 Pressure Drop Analyses . . . . .	8
II. PRESSURE LOSS COEFFICIENT FOR TUBE DRAG . . . . .	15
2.1 Introduction . . . . .	15
2.2 Theoretical Considerations . . . . .	15
2.3 Experimental Investigation . . . . .	20
2.4 Discussion of Results . . . . .	21
III. APPROXIMATE ANALYSIS OF SPRAY COOLERS . . . . .	25
3.1 The Problem . . . . .	25
3.2 The Design Model . . . . .	26
3.3 Evaluation of the Model . . . . .	35
IV. CONCLUSIONS AND RECOMMENDATIONS . . . . .	38
REFERENCES . . . . .	40
TABLES . . . . .	43
ILLUSTRATIONS . . . . .	48

## APPENDIXES

## I. TABLES

<u>Number</u>	
I. Values of Exponents $m$ , $n$ , and Constants $C_L$ and $C_G$ for Various Lockhart-Martinelli Combinations of Viscous and Turbulent Flows . . . . .	43
II. Test Conditions used in Tube Bank Pressure Drop Measurements . . . . .	44
III. Pressure Drop Data from J-5 Spray Cooler . . . . .	45
IV. Typical Solid Fuel Rocket Exhaust Composition . . . . .	46
V. "Noncondensable" Rocket Exhaust Gas Analysis . . . . .	47

## II. ILLUSTRATIONS

<u>Figure</u>	
1. Schematic Drawings of Flow Patterns in Horizontal Adiabatic Two-Phase Flow . . . . .	48
2. Schematic Drawings of Flow Patterns in Adiabatic Two-Phase Vertical Upflow . . . . .	49
3. Baker Flow Pattern Chart for Two-Phase Flow . . . . .	50
4. Results of Lockhart-Martinelli Correlation . . . . .	51

5.	Schematic of Flow Pattern in Tube Bank . . . . .	52
6.	Geometry of Initial Region of Free Jet, Showing Typical Velocity Profiles . . . . .	53
7.	Cross-Sectional View of Test Section for Air Flow Experiments . . . . .	54
8.	Typical Velocity Profiles at Various Stations in Tube Bank . . . . .	55
9.	Wall Static Pressure Distributions	56
10.	Generalized Wall Static Pressure Gradient as a Function of the Mass Flux . . . . .	57
11.	Relation Between Measured Velocity Profile and Average Velocity Between Adjacent Tubes . . . . .	58
12.	Ratio of Theoretical to Experimental Values of Pressure Loss Coefficient as a Function of Mass Flux . . . . .	59
13.	Comparison of Present Theory and Experimental Data With Results of Other Investigations of In-line Tube Banks .	60
14.	Spray Cooler Configuration for J-5 Rocket Test Facility . . . . .	61
15.	Control Volumes for Spray Cooler Analysis . . . . .	62
16.	Pressure Drop Ratio Versus Entrainment Parameter Parametric in Exhaust Inlet Temperature: Data Line 4.	63
17.	Pressure Drop Ratio Versus Entrainment Parameter Parametric in Exhaust Inlet Temperature: Data Line 5 .	64
18.	Pressure Drop Ratio Versus Entrainment Parameter Parametric in Exhaust Inlet Temperature: Data Line 6 .	65
19.	Pressure Drop Ratio Versus Entrainment Parameter Parametric in Exhaust Inlet Temperature: Data Line 8 .	66
20.	Pressure Drop Ratio Versus Entrainment Parameter Parametric in Exhaust Inlet Temperature: Data Line 9 .	67
21.	Pressure Drop Ratio Versus Entrainment Parameter Parametric in Exhaust Inlet Temperature: Data Line 10.	68
22.	Pressure Drop Ratio Versus Entrainment Parameter Parametric in Exhaust Inlet Temperature: Data Line 11.	69
23.	Pressure Drop Ratio Versus Entrainment Parameter Parametric in Exhaust Inlet Temperature: Data Line 12.	70
24.	Pressure Drop Ratio Versus Entrainment Parameter Parametric in Exhaust Inlet Temperature: Data Line 13.	71
25.	Pressure Drop Ratio Versus Entrainment Parameter Parametric in Exhaust Inlet Temperature: Data Line 14.	72
26.	Pressure Drop Ratio Versus Entrainment Parameter Parametric in Exhaust Inlet Temperature: Date Line 15.	73
27.	Pressure Drop Ratio Versus Entrainment Parameter Parametric in Exhaust Inlet Temperature: Data Line 16.	74
28.	Correlation of Droplet Entrainment Parameter with Ratio of Flow Energy Loss to Exhaust Outlet Mass Flow Rate .	75
29.	Effect of Pressure-Loss-Coefficient Constant on Pres- sure Drop Ratio as a Function of Entrainment Parameter: Data Line 13. . . . .	76

30.	Effect of Liquid Film Velocity on Pressure Drop Ratio as a Function of Entrainment Parameter: Data Line 13.	77
31.	Effect of Water Spray Injection Velocity on Pressure Drop Ratio as a Function of Entrainment Parameter: Data Line 13 . . . . .	78
32.	Effect of Cooling Water Flow Rate Supplied per Row of Spray Bars on Pressure Drop Ratio as a Function of Entrainment Parameter: Data Line 13 . . . . .	79

## NOMENCLATURE

A	Cross sectional area
$A_m$	Minimum frontal flow area
$A_1$	Local width of constant velocity jet core, $b_o - y_1$ (Fig. 6)
a	Parameter in equation (11)
b	Parameter in equation (11), also width of free shear layer in jet analysis of section II
$b_o$	Half-width of space between adjacent spray bars
C	Coefficient in equations (15) and (16)
$C_p$	Heat capacity
D	Hydraulic diameter
$D_p$	Pipe or duct diameter
d	Diameter of tube in spray bank
e	Kinetic energy rate
e'	Parameter defined in equation (38)
f	Fanning friction factor
G	Mass flux, mass flow per unit area
$g_c$	Gravitational constant
g	Gravitational acceleration
H	Enthalpy
h	Specific enthalpy
$h_{fg}$	Latent heat of vaporization
l	Reference length
M	Parameter defined in equation (24)
m	Exponent in equation (25)
$\dot{m}$	Mass flow rate
N	Parameter defined in equation (25)
n	Exponent in equation (15)
P	Fluid static pressure

$P_o$	Plenum stagnation pressure
$Q$	Volumetric flow rate in pipe
$q$	Volumetric flow rate in jet analysis
$\bar{R}$	Holdup parameter, average value over the pipe length
$R$	Holdup parameter, local value
$R_g$	Specific gas constant
$r$	Pipe radius
$Re$	Reynolds' number
$s$	Longitudinal center-to-center spacing of tubes in bank
$TD$	Tube drag
$u$	Local longitudinal velocity in tube bank
$u_j$	Maximum jet velocity in tube bank (Fig. 11)
$V$	Velocity
$\bar{V}$	Average velocity in pipe
$w$	Weight flow rate
$X$	Parameter defined in equation (21)
$x$	Longitudinal distance
$\bar{x}$	Parameter defined in equation (39)
$y$	Mole fraction in vapor phase
$y_1$	Location of core edge of free shear layer
$y_2$	Location of free edge of shear layer
$\alpha$	Void fraction
$\gamma$	Entrainment parameter, equation (51)
$\zeta$	Pressure loss coefficient in tube bank
$\eta$	Dimensionless width defined in equation (32)
$\theta$	Inclination angle from vertical
$\lambda$	Flowing liquid volume fraction $Q_L / (Q_L + Q_G)$
$\mu$	Fluid viscosity
$\rho$	Fluid density
$\tau_w$	Shearing stress at pipe wall

‡ Parameter defined in equation (17)

**SUBSCRIPTS**

a,b,c Arbitrary subscripts in equation (47)  
 cw Cooling water  
 d Liquid droplet  
 e Combined exhaust and steam flows  
 eff Effective  
 ex Exhaust gas  
 B Location of dividing streamline of free shear layer  
 G Gas phase  
 i Integer index for rows of spray bars: 1,2,3,....  
 L,l Liquid phase  
 li Liquid injected as spray  
 lf Liquid flowing, liquid film  
 m Mean value  
 n Integer index for control volumes: 1,2,3,....  
 N The last control volume  
 NS No slip, homogeneous flow (Dukler's Case I)  
 o Value at minimum area between two adjacent tubes in bank  
 s Steam  
 T Total combined exhaust and droplet flows  
 TP Two phase

## SECTION I GENERAL REMARKS

### 1.1 INTRODUCTION

In the performance testing of rocket propulsion systems under simulated high-altitude conditions, large amounts of hot combustion gas must be exhausted from the test cell and diffused to atmospheric pressure. Considerable cooling of these gases is necessary in order to reduce the volumetric flow rate as well as to protect containing surfaces. A common cooling technique involves the partial evaporation of water sprays which, while being both effective and relatively simple, results in the further requirement of separating the maximum possible amount of the water vapor and droplets from the cooled exhaust gas. The presence of water droplets is highly detrimental to rotary compressors, and more than the minimal amount of water vapor in the exhaust requires extra compressor capacity to achieve specified performance criteria.

The use of water sprays to cool hot exhaust gases gives a simultaneous flow of both gas and liquid phases in the exhaust ducts of rocket test cells. Such two-phase gas-liquid flow is a common occurrence in many other industrial processes, with boiling and condensing processes perhaps being the most familiar examples of two-phase flow processes. The transportation of oil, water, and gas simultaneously inside pipes is an integral part of the production and manufacture of petroleum and petrochemical products. Other two-phase flows which might be mentioned are the injection of liquid fuels into combustion chambers and the use of liquid films to cool the walls of rocket engines.

In all the two-phase flow processes mentioned above, the two phases involved are gas and the liquid phases. Two-phase flows could involve the flow of solid particles simultaneously with either a liquid or a gas, but reference in this report to "two-phase" flow will be restricted to flows involving only gas and liquid phases.

This report is concerned with the prediction of pressure drop across spray cooler sections contained within exhaust ducts of rocket test facilities used to evaluate rocket performance at simulated high altitudes. In the first portion of this report, the current state of theoretical approaches to the general problem of two-phase flow is reviewed. These analyses presume fully developed flow conditions as a simplifying assumption, a condition not fulfilled in the operation of these spray coolers. The spray coolers considered here are only a few duct diameters in length, and the flows are thus confined to the

developing flows characteristic of entrance regions. However, the summary of current two-phase flow theory will provide background knowledge for consideration of the more complex problems encountered in these spray coolers.

The discussion in Section II includes experimental results to improve estimation of the pressure loss coefficient in subsequent expressions for the pressure drop associated with tube drag. The necessity encountered was one of specializing a previous analysis to the particular geometry of the J-5 spray cooler located at AEDC.

In Section III a mathematical model for the design of spray coolers is presented. Test firing data were then used to assess certain features of the model. Based on these evaluations, a correlation was obtained for the "droplet entrainment parameter" contained in the model.

## 1.2 PRESENT STATE OF KNOWLEDGE

Because of the large number of publications which have appeared concerning two-phase flow, a comprehensive review of the literature will not be presented in this report. Instead, a brief survey of the two-phase flow literature will be given, with descriptions of particular work included only if the work represents a significant advance or is pertinent as background to the analysis presented in this report. The reader is referred to Ref. 1-6 for more detailed reviews of two-phase flow, of which Ref. 1-5 also contain extensive bibliographies on the subject. References 7-9 are entirely bibliographies on two-phase flows, and Ref. 10 gives an extensive treatment on the injection and combustion of fuels. The work by Gouse (Ref. 7) containing 5253 entries represents the largest and most recent of the bibliographies, whereas Kepple and Tung have compiled in Ref. 8 an especially useful bibliography of 2843 entries, each containing an abstract of the reference.

The science of fluid mechanics has evolved mainly through the study of single-phase flow. The effort expended over a great many years has given an understanding of single-phase flow sufficient for analysis and design work in many situations. Because many processes of economic and technical importance involve two-phase flow, there is a similar motive to develop an equally good understanding of two-phase flow. However the complexity of two-phase flow, as contrasted to single-phase flow, has caused the understanding of such flow to be much less complete than of single-phase flow.

To illustrate the complexity of two-phase flow relative to single-phase flow, recall that the prediction of friction pressure loss depends on five variables: Fluid density, fluid viscosity, fluid velocity, pipe diameter, and pipe wall roughness. Furthermore, the flow may be characterized as laminar or turbulent, depending simply on the magnitude of the Reynolds number. However, the

friction pressure loss in two-phase flow has been found to depend on the viscosity, density, and velocity of each phase, pipe diameter, pipe wall roughness, surface tension at the gas-liquid interface, local acceleration of gravity, and the angle of inclination of the flow direction. Thus, there are eleven independent parameters upon which friction pressure drop depends in two-phase flow as contrasted to five for single-phase flow. The number of dimensionless groups required to relate the variables in two-phase flow is nine, whereas only three are needed for single-phase flow. Such a large number of independent variables makes it a formidable task to obtain a general correlation by dimensional analysis and experimental measurements. Although certain dimensionless groups appear in most correlations, a generalized friction pressure drop correlation based primarily on dimensional analysis has not yet appeared.

Although the concept of a critical Reynolds number is sufficient in single-phase flow to define the transition from laminar to turbulent flow, the case for two-phase flow is much different. Two-phase flow cannot be so simply classified into these two flow regimes which characterize single-phase flow because the liquid and gas phases are distributed over the conduit cross-section in different ways depending on the flow conditions, and each phase may flow laminarily or turbulently. Thus, a simple Reynolds number criterion alone is insufficient to specify the type of flow because it does not take into account the phase distributions which occur for different conditions of two-phase flow. However, despite the relative complexity of two-phase flow as compared to single-phase flow, investigations over the last two decades have achieved improved understanding of these flow phenomena.

### 1.3 FLOW PATTERNS

The distributions of phases or "flow patterns", as mentioned above, are an important consideration from a fundamental standpoint to a meaningful description of two-phase flow behavior. Although solutions based on mathematical models for a particular flow pattern have not been generally of much greater accuracy than those which ignore the flow pattern, it is usually acknowledged that each flow pattern must be analyzed separately to predict pressure drop accurately in two-phase flow. The failure of flow pattern models to predict friction pressure drop with greater accuracy can be attributed in part to the real difficulty in describing the flow structure in detail. At present such detailed mathematical descriptions of the flow structure are not available. Thus, the simplifying assumptions and approximations made to give a tractable mathematical model cause the predicted friction pressure drops to deviate from the actual values.

Another problem inherent in the use of flow pattern models is that of predicting what flow pattern will exist for a given set of flow conditions. No quantitative means for defining flow patterns now exists, and flow patterns descriptions are based on visual observation of the phase distributions through transparent sections in a flow conduit. Because the results of flow pattern experiments are reported as verbal descriptions of visual observations, descriptions and designations of flow patterns reported by different investigators vary. Moreover, the transition from one flow pattern to another as flow conditions are changed is gradual, not abrupt. A particular distribution of the phases may be considered as distinct by some investigators while others might regard this same distribution as a transition zone between other flow patterns.

The flow patterns shown in Figure 1 represent a frequently used set of flow pattern classifications for horizontal flow. Because the boundaries between patterns are difficult to define, some of the flow patterns shown might be considered merely as transition patterns. For example, wavy flow might be considered as the transition from stratified to slug flow. Spray flow could be considered the limiting case of annular flow (very thin liquid film on the pipe wall). Alternatively, more classifications than those shown in Figure 1 have been presented; Knowles et al. (Ref. 11) proposed twelve flow patterns for horizontal adiabatic flow. Similarly, one set of flow patterns which has been delineated for adiabatic vertical upflow is shown in Figure 2. Note that the stratified and wavy patterns do not exist for vertical flow.

All attempts to predict which flow pattern will exist for a given set of flow conditions have been based on empirical correlations of experimental data, the most widely used correlation being the well-known "Baker Flow Pattern Chart" for horizontal flow (see Fig. 3 and Ref. 12). Notice that Baker used the term "dispersed" flow for "spray" flow (also called "mist" flow by some investigators). Baker also emphasized that the boundaries between the flow patterns are not really lines, as shown on the chart, because the transition from one flow pattern to another is gradual. As expected, the sequence of flow patterns which can exist depends upon both the gas flow rate and the liquid flow rate. A number of other flow pattern charts which have been developed are also described in (Ref. 12).

A characteristic common to all flow pattern correlations is that each will predict flow patterns correctly for some flow conditions, but not for others. This discrepancy between predicted and observed flow patterns may be attributed to the facts that (1) flow patterns are classified according to visual observations, the

boundaries between flow patterns not being well defined, (2) most correlations do not include all the pertinent independent variables, (3) the correlations are based on data for only a limited range of flow conditions.

To refine flow pattern predictions further, a quantitative and measurable parameter which characterizes the flow pattern must be found. Some effort has been directed toward such quantitative flow pattern characterization (Ref. 13), but this work is yet at an early stage and no general correlations have emerged.

#### 1.4 PRESSURE DROP

The momentum integral equation for steady upward flow within a circular pipe (inclined at an angle  $\theta$  to the vertical) is

$$\frac{dP}{dx} = - \frac{4\tau_w}{D_p} - \frac{8}{D_p^2 g_c} \frac{d}{dx} \int_0^{D_p/2} \rho v^2 r dr - \frac{8g \cos \theta}{D_p^2 g_c} \int_0^{D_p/2} \rho r dr \quad (1)$$

The first term on the right hand side of equation (1) represents the friction contribution to pressure drop, the second gives the acceleration contribution, and the third expresses the gravitational contribution.

In one-dimensional single-phase flow the friction factor concept is typically used to represent the wall shear stress in the friction pressure drop term. With the introduction of the Fanning friction factor,

$$f = \tau_w / (\rho v^2 / 2g_c) \quad (2)$$

the friction pressure-drop term becomes

$$-2\rho \bar{V}^2 f / (g_c D_p) \quad (3)$$

For one-dimensional single-phase flow the acceleration term is

$$- \frac{(4w)^2}{(\pi D_p^2)^2 g_c} \frac{d(1/\rho)}{dx} \quad (4)$$

and the gravity term is

$$- (\rho g / g_c) \cos \theta \quad (5)$$

With these simplifications the total pressure drop is expressible as

$$\frac{dP}{dx} = \frac{-2\rho\bar{v}^2 f}{D_p g_c} - \frac{(4w)^2}{(\pi D_p^2)^2 g_c} \frac{d(1/\rho)}{dx} - \frac{\rho g \cos \theta}{g_c} \quad (6)$$

Note that  $\cos \theta = 0$  for horizontal flow, and also that the acceleration term is zero for an incompressible fluid. For a compressible fluid the density can be expressed in terms of the fluid pressure and temperature by an equation of state. Thus, in single phase flow, the above equation can be used to determine friction factors based on experimental measurements of total pressure drop. Conversely, once the friction factor has been correlated to pertinent flow parameters in a general manner, total pressure drop can be calculated from the same correlation.

For two-phase flow, the simplifications that were possible for single-phase flow cannot be applied. In single-phase flow the acceleration contribution to pressure drop results from the expansion of a compressible fluid as the pressure decreases along the conduit. In two-phase flow the gas phase expands as the pressure is reduced, but the phase distribution also changes and evaporation or condensation will change the cross-sectional areas occupied by the two phases, thus causing an additional acceleration contribution.

If a two-phase flow is created by the mixing of a liquid and a gas, there is an acceleration contribution to the pressure drop as the phase distribution undergoes changes until a quasi-equilibrium distribution is reached. The movement of liquid within that phase from a region of low velocity to a region of higher velocity, or vice-versa, causes an acceleration of that fluid. The term quasi-equilibrium is used to acknowledge that phase distribution is always changing in the axial direction (even in the absence of evaporation, condensation, or entrance effects) because the phase distribution is influenced by gas phase density, which is dependent on pressure. Thus, with the continuous decrease in pressure in the flow direction there is a concomitant and continuous change in the phase distribution. For some flow conditions, such as those at high pressures, small liquid flow rates, or in large diameter pipes, the acceleration contribution to the pressure drop may be small, whereas the acceleration contribution has been shown to be large (Ref. 14) for flows at low pressures or in small diameter pipes.

The gravitational contribution to pressure drop in two-phase flow can be determined only if the density of the two-phase mixture is a known function of the radial coordinate. Thus, the gravity contribution, like the acceleration contribution, is significantly dependent upon the phase distribution or flow pattern.

The "holdup" parameter ( $R_L$ ), which is frequently encountered in the two-phase flow literature, is also closely related to phase distribution. Holdup is defined as the fraction of the total cross-sectional area occupied by the liquid phase under actual flow conditions. It should be noted that holdup is not simply equal to the ratio of liquid volume flow rate to total volume flow rate, even on an average basis ( $\bar{R}_L$ ).

While total pressure drop measurements can be made for two-phase flows, the changes in phase distribution and local phase velocities required for evaluating the acceleration and gravitational contributions to pressure drop are extremely difficult to measure. For this reason, very little of the pressure drop data available today for two-phase flow includes information which would permit even a very crude approximation of the acceleration contribution. Experimental data on liquid holdup permit only approximate values for the acceleration and gravity terms to be calculated.

Many of the early experimenters underestimated the magnitude of the acceleration term and believed it to be negligible; consequently, the friction factor correlations developed were based on total pressure drop instead of friction pressure drop. Unless the correlation between the friction pressure drop and the flow variables is the same as that between the acceleration pressure drop and the flow variables, a correlation of friction factor to total pressure drop cannot accurately predict total pressure drop under flow conditions which produce acceleration pressure drops different from those in the experiments from which the correlation was obtained.

Another factor not considered in many of the early experiments is the "entrance length" required for the phase distribution to reach a quasi-equilibrium state. Acceleration effects are significant in the entrance region, and both acceleration pressure drop and friction pressure drop are functions of the phase distribution immediately after mixing. Because changes of phase distribution in the entrance region depend on how the two phases are mixed, the method of mixing becomes an additional independent variable if pressure drop measurements are taken too close to the mixing point. Effects of the method of mixing have been observed as much as 220 pipe diameters downstream of the mixing point (Ref. 15).

## 1.5 PRESSURE DROP ANALYSES

Many experimental measurements of pressure-drop have been made to date, and most investigators have presented equations based on their data to predict pressure drop. The many empirical correlations will not be discussed here because, for the most part, they are reliable only for flow conditions identical to those in the experiment from which they were obtained. Instead, four semi-empirical analyses will be discussed which typify different approaches to the problem of pressure drop prediction.

### Homogeneous Model

The study of the fluid mechanics of two-phase flow has advanced primarily through the application and extension of principles developed in single-phase flow. The homogeneous model, which is considered in detail in Ref. 2, represents the most direct application of single-phase flow principles to two-phase flow in that the model assumes that both phases are distributed uniformly over the pipe cross-section and that both phases flow with the same velocity. With these assumptions the two-phase mixture is treated as a single-phase fluid with average properties for the mixture. Although various definitions for the mixture properties have been proposed, the similarity analysis of Dukler et al. (Ref. 16) shows that the correct mixture properties consistent with the assumptions of the homogeneous model are given by:

$$\rho = \rho_L \lambda + \rho_G (1-\lambda) \quad (7)$$

$$\mu = \mu_L \lambda + \mu_G (1-\lambda) \quad (8)$$

Equation (6) can be used to predict two-phase pressure drop based on the homogeneous model if the density and viscosity terms are taken to be the mixture density and the mixture viscosity. The friction factor is correlated to the mixture Reynolds number just as friction factors are correlated to Reynolds number in single-phase flow. The flow patterns shown in Figures 1 and 2 suggest that the homogeneous model will be more applicable to bubble and spray flows since these phase distributions are more nearly homogeneous than the others. In general, however, the homogeneous models have been unsuccessful in predicting pressure drops accurately over a wide range of flow conditions.

### Lockhart-Martinelli Model

The most widely used correlation is that of Lockhart and

Martinelli (Ref. 17). Their model accommodates the nonhomogeneous distribution of the two phases over the cross-sectional area and also different phase velocities. The basic postulates upon which the model is based are quoted as:

1. "Static pressure drop for the liquid phase must equal the static pressure drop for the gaseous phase regardless of the flow pattern, as long as an appreciable radial static pressure difference does not exist."
2. "The volume occupied by the liquid plus the volume occupied by the gas at any instant must equal the total volume of the pipe."

Moreover, each phase is considered to flow separately with its own velocity and flow area, and it is supposed that the pressure drop in each phase can be obtained from equations for single-phase flow using the familiar Fanning friction factor approach.

Because the two phases are considered to flow independently, one can write

$$W_L = \rho_L A_L V_L \quad (9)$$

and

$$W_G = \rho_G A_G V_G \quad (10)$$

where the velocities  $V_L$  and  $V_G$  are average velocities for the two phases. The cross-sectional flow areas are  $A_L$  and  $A_G$  for the liquid and gas phases, respectively, and these are related to the "hydraulic diameters"  $D_L$  and  $D_G$  by

$$A_L = a \left( \frac{\pi D_L}{4} \right) \quad (11)$$

$$A_G = b \left( \frac{\pi D_G}{4} \right) \quad (12)$$

The parameters  $a$  and  $b$  depend on the phase distribution.

Neglecting acceleration and gravitational contributions, the pressure drop equation expressed in terms of either phase is

$$\left( \frac{dP}{dx} \right)_{tp} = - \frac{2 \rho_L V_L^2 f_L}{D_L g_c} \quad (13)$$

or

$$\left(\frac{dP}{dx}\right)_{tp} = - \frac{2\rho_G V_G^2 f_G}{D_G g_C} \quad (14)$$

The friction factors are assumed to be expressible in the Blasius form:

$$f_L = C_L (Re_L)^{-n} = C_L \left( \frac{4W_L}{\pi a D_L \mu_L} \right)^{-n} \quad (15)$$

$$f_G = C_G (Re_G)^{-m} = C_G \left( \frac{4W_G}{\pi b D_G \mu_G} \right)^{-m} \quad (16)$$

where the values of  $C_L$  and  $n$  or of  $C_G$  and  $m$  depend upon whether the flow is laminar or turbulent. Combining equations (9,11,13, and 15) gives

$$\frac{\left(\frac{dP}{dx}\right)_{tp}}{\left(\frac{dP}{dx}\right)_L} = a^{n-2} \left(\frac{D_P}{D_L}\right)^{5-n} = \frac{2}{L} \quad (17)$$

where

$$\left(\frac{dP}{dx}\right)_L = \frac{2 \left(\frac{4}{\pi}\right)^{2-n} C_L \mu_L^n W_L^{2-n}}{D_P^{5-n} \rho_L g_C} \quad (18)$$

Similarly, combining equations (10,12,14, and 16) gives

$$\frac{\left(\frac{dP}{dx}\right)_{tp}}{\left(\frac{dP}{dx}\right)_G} = b^{m-2} \left(\frac{D_P}{D_G}\right)^{5-m} \quad (19)$$

where

$$\left(\frac{dP}{dx}\right)_G = \frac{2 \left(\frac{4}{\pi}\right)^{2-m} C_G \mu_G^m W_G^{2-m}}{D_P^{5-m} \rho_G g_C} \quad (20)$$

Note that  $(dp/dx)_L$  is just the expression for pressure drop for liquid flow alone in the pipe, and  $(dp/dx)_G$  is the pressure drop for single-phase gas flow.

Lockhart and Martinelli assumed that the parameters  $\phi_L$  and  $\phi_G$  are only functions of the parameter

$$X = \frac{\left(\frac{dP}{dx}\right)_L}{\left(\frac{dP}{dx}\right)_G} \quad (21)$$

and used  $X$  to correlate values of  $\phi_L$  and  $\phi_G$  obtained from experimental pressure drop measurements.

Lockhart and Martinelli postulated that the flow of each phase could be either laminar or turbulent; thus, they were able to define four flow mechanisms:

- 1) turbulent flow of both phases (turbulent-turbulent)
- 2) laminar liquid flow and turbulent gas flow (viscous-turbulent)
- 3) turbulent liquid flow and laminar gas flow (turbulent-viscous)
- 4) laminar flow of both phases (viscous-viscous)

The flow of a phase was arbitrarily assumed to be laminar if the Reynolds number based on the pipe diameter was less than 1000 and turbulent if the Reynolds number was greater than 2000. Values of  $C_L$ ,  $C_G$ ,  $m$  and  $n$  for the various flow types are given in Table 1.

Figure 4 shows the results of the Lockhart-Martinelli correlation for the four cases noted above. These curves can be used to predict pressure drop correctly to within about  $\pm 60$  percent over a wide range of flow conditions, and their model has been used primarily because of its wide range of applicability.

Certain limitations of the Lockhart-Martinelli analysis should be mentioned. The definition of the four flow types is arbitrary. Furthermore, the correlation does not account separately for the acceleration contribution to pressure drop. The assumption that  $\phi_L$  and  $\phi_G$  are functions of  $X$  alone has been shown to be incorrect, as has the assumption that the pressure drop for the separate phases can be expressed using single-phase flow equations. However, in a subsequent work based on an annular flow pattern and assumed velocity profiles, Levy (Ref. 18) determined an analytical relationship between  $\phi_L$ ,  $\phi_G$  and  $X$ .

#### Similarity Analysis

Dukler et al. (Ref. 16) applied the principle of similarity to two-phase flow and found that correct expressions for the friction

factor and Reynolds number are:

$$f_{tp} = \frac{1}{2} \frac{dP/dx}{\bar{V}_m^2 / g_c \ell} \left[ \rho_L \frac{\lambda^2}{\bar{R}_L} + \rho_G N \frac{(1-\lambda)^2}{\bar{R}_G} \right]^{-1} \quad (22)$$

$$Re_{tp} = \ell \bar{V}_m \frac{(\rho_L \lambda^2 / \bar{R}_L) + (\rho_G N (1-\lambda)^2 / \bar{R}_G)}{\mu_L \lambda + \mu_G (1-\lambda) N} \quad (23)$$

where

$$\bar{V}_m = (Q_L + Q_G) / A_t$$

$$M = \frac{R_G}{\bar{R}_G} \frac{\bar{R}_L}{R_L} \left( \frac{\bar{V}_L}{\bar{V}_G} \right)^2 \frac{V_G}{V_L} \frac{dV_G / dx}{dV_L / dx} \quad (24)$$

$$N = \frac{R_G}{\bar{R}_G} \frac{\bar{R}_L}{R_L} \frac{\bar{V}_L}{\bar{V}_G} \frac{d^2 V_G / dr^2}{d^2 V_L / dr^2} \quad (25)$$

Because the quantities M and N as well as  $\bar{R}_L$  and  $\bar{R}_G$  are obviously not known, the friction factor and Reynolds number expressions are of little use in these forms. However, Dukler et al. obtained simpler expressions for friction factor and Reynolds number for two cases:

**Case I:** Local phase velocities are equal (no slip) and the flow is homogeneous. This case is identical to the homogeneous flow model discussed previously. With these assumptions equations (22) and (23) reduce to

$$f_{ns} = \frac{dP}{dx} \left[ 2 \left( \frac{4W_t}{\pi D_p} \right)^2 / \rho_{ns} D_p g_c \right]^{-1} \quad (26)$$

$$Re_{ns} = \frac{4W_t}{\pi D_p \mu_{ns}} \quad (27)$$

where  $\rho_{NS}$  and  $\mu_{NS}$  are given by equations (7) and (8) and  $l = D_p$ .

**Case II:** Local phase velocities are not equal but M and N are assumed to be unity. These assumptions give

$$f_{tp} = f_{ns} \left[ \left( \frac{\rho_L}{\rho_{ns}} \right) \frac{\lambda^2}{\bar{R}_L} + \left( \frac{\rho_G}{\rho_{ns}} \right) \frac{(1-\lambda)^2}{\bar{R}_G} \right]^{-1} \quad (28)$$

$$Re_{tp} = Re_{ns} \left[ \left( \frac{\rho_L}{\rho_{ns}} \right) \frac{\lambda^2}{\bar{R}_L} + \left( \frac{\rho_G}{\rho_{ns}} \right) \frac{(1-\lambda)^2}{\bar{R}_G} \right] \quad (29)$$

In this case  $\bar{R}_L$  is presumed available from a correlation for holdup.

For Case I, the relationship between friction factor and Reynolds number was taken to be the same as that for single phase flow, viz.,

$$f_{ns} = 0.0014 + 0.125 (Re_{ns})^{-0.32} \quad (30)$$

For Case II, the ratio  $f_{tp} / f_o$  (where  $f_o$  is obtained from equation (30) using  $Re_{tp}$  from equation (29) for  $Re_{ns}$ ) was correlated to  $\lambda$  using friction pressure drops obtained from extensive experimental data. These friction pressure drops were obtained from total pressure drops values of the acceleration and gravitational contributions estimated from calculated holdup data. Based on a statistical comparison of Case I, Case II, and the Lockhart-Martinelli analysis, Dukler concluded that the Case II correlation shows better agreement with the data in most cases.

The work of Dukler et al. is significant not only because it represents the first formal application of similarity analysis to two-phase flow, but because the Case II correlation is based on over 400 experimental data points covering a wide range of flow conditions.

#### Levy's Mixing Length Analysis

None of the analyses mentioned previously attempt to describe the local behavior of the two phases. Levy (Ref. 19) adapted the well-known mixing length concepts of turbulent single-phase flow to predict pressure drop in two-phase flow. Levy assumed that the two-phase flow can be represented by a mixture whose density varies continuously along the radial co-ordinate. The mass transfer component of the turbulent shear stresses was retained in the expression for the

Reynolds stresses. The fluctuating velocity and density components were related to the average velocity and density gradients using the Van Driest modification of Prandtl's mixing length theory. The mixing length for a mass transfer was assumed equal to that for momentum transfer. Thus, the mixing length equations plus a potential flow equation relating local time average values of the velocity and density gave an ordinary differential equation which could be solved numerically to obtain the density distribution over the flow cross-sectional area. Friction factors were predicted in terms of a mean density and a Reynolds number based on total flow rate and liquid viscosity. The mean fluid density was related empirically to known flow variables using experimental data.

Levy's mixing length model shows acceptable agreement with experimental data only for a limited range of the flow conditions. However the mixing length model is an important contribution to improved understanding of two-phase flow because it treats such flow on a local basis using the conservation equations. The inadequacy of the pressure drop predictions can be attributed to the many simplifying assumptions which were made necessary by the present lack of knowledge of these local conditions.

In summary, it may be said that although a certain understanding of fundamental aspects of relatively simple two-phase flow behavior does exist, current knowledge is insufficient to permit accurate prediction of pressure drops associated with the concomitant problems of handling and cooling large volumes of hot rocket exhaust gases by use of water sprays. Consequently, other approaches described in the subsequent sections of this report were undertaken.

## SECTION II

### PRESSURE LOSS COEFFICIENT FOR TUBE DRAG

#### 2.1 INTRODUCTION

The problem of specifying the pressure drop coefficient to fix the pressure loss associated with flow over the spray bar array is considered in this section. There is apparently no previous work sufficient to describe uniquely the situation encountered within the spray cooler problem. Although pressure losses caused by flow over tube banks have been long studied as part of the design of certain types of heat exchangers and similar configurations, none of these studies has considered the spray bar problem pertinent to this investigation. The bulk of the available data on pressure drop across tube banks resulted from experimental studies prior to 1940, with another surge of information being generated in the early 1940's because of World War II. Typical of the latter works are those published as NACA Wartime Reports (Refs. 20 and 21, for example).

The approach to this part of the spray cooler problem will be to modify the method given by Abramovich (Ref. 22) for predicting pressure loss with single-phase flows over tube banks, and subsequently, to incorporate it in the model to be given for the design of spray cooler sections. Some theoretical aspects of the analysis for the tube drag associated with single-phase flows will be considered first. Following this, results of some experimental work done as a part of this investigation to assess the validity of theory and to specialize results to the spray cooler geometry considered here will be presented. Additional details of this portion of the investigation may be found in Ref. 23.

#### 2.2 THEORETICAL CONSIDERATIONS

A theoretical estimate of the static pressure loss across a tube bank can be obtained with a method presented by Abramovich (Ref. 22). In this flow model the pressure loss caused by the tube bank is considered to result from the difference in the kinetic energy of the flow between a bar located at station 1 in Fig. 5 and a position just ahead of the next row of bars (station 1'). The difference in kinetic energy appears as a pressure loss, because the flow must accelerate to pass through the next row of bars. This loss in total kinetic energy of the jet is due to mixing of the relatively high velocity fluid in the core of the jet with the low speed flow which circulates in the wake region behind the bars.

In determining the kinetic energy losses, the following assumptions are made about the flow: (1) there is uniform velocity at stations 1 and 2; (2) the region between 1 and 1' is isobaric;

(3) there is no interaction between the flow passing between adjacent pairs of bars; (4) the flow is incompressible.

As the fluid passes between a pair of bars, viscous effects cause the jet-like flow to grow in width, and a mixing zone or free shear layer is formed at each edge of the jet. As the mixing regions spread, the average velocity of the flow is reduced. The core is eventually dissipated by viscous action and the two shear layers merge at some point B (See Fig. 6).

The effective "edges" of the shear layer (See Fig. 6) were shown by Abramovich to be given by  $y_1/b = 0.416$  and  $y_2/b = 0.584$ . That is, the inner portion of the mixing zone grows slightly slower than the outer layer. The development, which is omitted for brevity, is based on approximations to the continuity and momentum equations (See Ref. 22, Chapter 4, page 148).

The thickness of the free shear layer has been found experimentally to increase linearly with the axial distance,  $x$ , (See Fig. 6) and is given by  $b = 0.27x$ . The corresponding velocity profile in the mixing zone has also been determined experimentally and may be approximated by the polynomial given in Schlichting (Ref. 24):

$$\frac{u}{u_0} = 2\eta^{1.5} - \eta^3 \quad (31)$$

where

$$\eta = \frac{y-y_2}{y_1-y_2} = \frac{y-y_2}{b} \quad (32)$$

and  $u_0$  is the core velocity.

To determine the energy of the jet at any longitudinal station, one must first establish the boundaries of primary flow (i.e., the flow which passes between the bars at station 1). This boundary is known as the dividing streamline since it separates induced and primary streams. The volumetric flow rate for the half-jet at station 1 is

$$q_1 \sim u_0 b_0$$

whereas at any longitudinal station the same volumetric flow rate is

$$q \sim \int_0^{y_B} u dy + \int_{y_1}^0 u dy + u_0 A_1$$

where  $A_1$  is the width of the constant velocity core and  $y_B$  is the location of the dividing streamline. But from Fig. 6 it is evident that  $A_1 = b_o - y_1$ , so that

$$q \sim \int_{y_1}^{y_B} u dy + u_o (b_o - y_1)$$

Hence, the ratio of the flow rates yields

$$\frac{q}{q_1} = \frac{u_o (b_o - y_1) + \int_{y_1}^{y_B} u dy}{u_o b_o}$$

or

$$\frac{y_1}{b} = \frac{1}{b} \int_{y_1}^{y_B} \frac{u}{u_o} dy = \frac{y_2 - y_1}{b_o} \int_{y_1}^{y_B} \frac{u}{u_o} \frac{dy}{y_2 - y_1} \quad (33)$$

But from equation (32)

$$\frac{dy}{y_2 - y_1} = d\eta$$

so that, after substitution of equation (31) and the foregoing relation into equation (33) one obtains

$$\begin{aligned} \frac{y_1}{b_o} &= \frac{y_2 - y_1}{b_o} \int_{\eta_B}^1 (2\eta^{1.5} - \eta^3) d\eta \\ &= \frac{b}{b_o} (0.55 - 0.8\eta_B^{2.5} + 0.25\eta_B^4) \end{aligned} \quad (34)$$

However, as was noted in the beginning  $y_1/b = 0.416$ , thus

$$0.8\eta_B^{2.5} - 0.25\eta_B^4 = 0.134$$

which yields the location of the dividing streamline as

$$\eta_B = \frac{y_B - y_2}{b} = 0.515 \quad (35)$$

Now, with the dividing streamline known, the energy loss due to viscous mixing may be estimated. At station 1 the initial kinetic energy of the jet is

$$e_1 \sim \rho_o u_o^3 b_o \quad (36)$$

whereas at an arbitrary location, the kinetic energy of that flow between the dividing streamlines is

$$e \sim \rho_o u_o^3 A_1 + \rho_o \int_{y_1}^{y_B} u^3 dy \quad (37)$$

Thus, the ratio of the two energy terms is

$$e' = \frac{e}{e_1} = \frac{A_1}{b_o} + \frac{y_2 - y_1}{b_o} \int_{\eta_B}^1 \left( \frac{u}{u_o} \right)^3 \frac{dy}{y_2 - y_1} \quad (38)$$

or

$$\begin{aligned} e' &= \frac{b_o - y_1}{b_o} + \frac{b}{b_o} \int_{0.515}^1 (2\eta^{1.5} - \eta^3)^3 d\eta \\ &= 1 - 0.092 b/b_o \end{aligned}$$

But  $b = 0.27x$  so that

$$e' = 1 - 0.025 \bar{x} \quad (39)$$

where  $\bar{x} = x/b_o$ . Between stations 1 and 1' with longitudinal bar spacing  $S$  (See Fig. 5), the ratio is

$$e' = 1 - 0.25 \frac{S}{b_o} \left( 1 - \frac{d}{2S} \right) \approx 1 - 0.025 S/b_o \quad (40)$$

because  $d/2S \ll 1$  in the present case. Thus, the change in the kinetic energy ratio is

$$\Delta e' = \frac{e_1 - e'}{e_1} = 0.025 s/b_o = 0.025 \bar{s} \quad (41)$$

The pressure drop can be related to the kinetic energy loss in the following manner. Let  $\Delta e' = \zeta$ . Then

$$\zeta = \frac{\dot{m} \Delta u^2}{\dot{m} u_o^2}$$

From the steady-flow energy equation it is noted that

$\Delta P/\rho \sim \Delta u^2/g_c$ , and hence,

$$\zeta = g_c \Delta P / \rho u_o^2 \quad (42)$$

or

$$\Delta P = \zeta \rho u_o^2 / g_c \quad (43)$$

where

$$\zeta = 0.025 (s/b_o) \quad (44)$$

If the pressure gradient is uniform from row to row, the pressure drop for  $n$  rows of tubes may be determined by multiplying the above expression by  $n$ . This result when combined with equation (41) gives

$$(\Delta P)_n = \frac{\zeta n}{g_c} \rho u_o^2 = \frac{0.025n}{g_c} \left( \frac{s}{b_o} \right) \rho u_o^2 \quad (45)$$

The  $\rho u_o^2$  term will be specialized to the two-phase flow analysis in Section III, but the concern at this point is whether or not the value of the constant (0.025) is appropriate for the spray cooler geometry. The analysis given above has presumed a uniform array of tubes of a constant diameter. This is not the case for the J-5 cooler, which was used in this work as a typical or example cooler configuration. Thus, the assessment of the validity of the theoretical value of 0.025 for the constant was necessary and done by

recourse to the experimental work described below.

### 2.3 EXPERIMENTAL INVESTIGATION

A series of experiments was made on a scale model of the AEDC J-5 spray bar configuration. The model was constructed with wall static taps at several points along the tube bank to determine the effect of upstream constrictions on the local pressure loss as well as to determine the overall pressure loss. Also, provision was made for taking velocity profiles both ahead of and behind various rows of bars to obtain a description of the flow field.

Test data were obtained from a tubular test cell, fitted between conical diverging and converging sections (See Fig. 7). The test cell was fabricated from plexiglass and was secured between the two variable-area sections by three axial bolts which ran the length of the test section. Aluminum plates on either end of the test section, along with the bolts, held the test section in place and served to seal the chamber against leakage. The rectangular array of bars inside the test section was fabricated from brass rod and held in place by clear epoxy cement.

Static pressure taps were installed at various stations along the walls of the test section. The taps were made of 0.050-inch diameter steel hypodermic tubing, and were pressed into the wall with an interference fit. At the inside wall of the test section, the tap diameter was 0.025 inches.

At the same longitudinal location of each static pressure tap, but displaced from it by  $90^{\circ}$ , were two additional sets of holes through the wall which were provided to facilitate pitot tube traverses directly behind a row of bars, and directly in front of the adjacent row of bars. The pitot tube used for these velocity profile measurements was also fabricated from 0.050-inch diameter stainless steel hypodermic tubing. One end of the tubing was closed, and a 0.025 inch hole was drilled into and perpendicular to the wall near the midpoint of the tubing.

The pitot tube was calibrated against a standard Prandtl impact tube over the anticipated range of velocities. As would be expected, there was some error due to local crossflow effects when the tube was in a steep transverse velocity gradient. However, this was not considered to be of major consequence even though such gradients exist in the flow field. Traverses were operated with a micrometer lead screw mechanism having forty threads per inch.

The test apparatus consisted of a plenum chamber, test section, pitot tubes, and manometers. The test section was preceded with a

six-foot length of 1.25 inch diameter copper pipe to assure fully developed, turbulent, parallel flow. The plenum chamber was fed from a receiving tank which, in turn was supplied by a two-stage reciprocating compressor. The air was passed through two porous stone filters for dehumidification before it reached the plenum chamber. Maximum stagnation pressure and temperature obtainable in the chamber were 100 psig and 130°F, respectively. The maximum flow rate of this compressor is approximately 1.0 lbm/sec.

All pressures were recorded on two 100-inch U-tube mercury manometers which were coupled in series. One leg of each manometer was pressurized by a house compressor and the unknown pressure (probe or static) was fed into the one leg, while the fourth leg was left open to the atmosphere. This technique permitted measurement of gage pressures up to 200 inches Hg.

Flow rates were determined from integration of measured velocity profiles which were obtained immediately upstream of the first row of bars. These flow rates, which covered the range of compressor capacity, were plotted against the plenum chamber pressure to form a calibration curve for the test apparatus.

As noted previously, transverse profiles of velocity were obtained just after the flow passed between a given row of bars (i.e., immediately upstream of a static pressure tap) and just before entering the reduced flow area at the next row of bars. These profiles were taken approximately 0.025 inches behind the trailing edge of the upstream row of bars and 0.075 inches ahead of the downstream row of bars. Traverses were started at the wall and readings were taken at the maximum and minimum velocity points over approximately the first 0.60 inches. Readings were taken at 0.025 inch increments across the center portion of the test section, to a point approximately 0.60 inches from the opposite wall.

Because visual distortion through the curved surface of the plexiglass tube prevented accurate positioning of the pitot tube at the wall, the center spray bar was used as a reference point from which transverse distances were measured. From the center bar the pitot tube was translated by an amount equal to the test section radius and this position was taken as the effective wall location. The inherent inaccuracy in this method and the slack in the lead screw mechanism made a slight translation of the velocity distributions necessary when the profiles were plotted.

## 2.4 DISCUSSION OF RESULTS

Typical velocity profiles found at various stations in the test cell are shown in Fig. 8. Also indicated on this plot is the relative position of the bars in the flow field. The base line of the

velocity profile corresponds to the location of the probe. It is observed that the profiles exhibit the expected jet-like peaks just downstream from each row of bars. The actual distributions are seen to be nearly parabolic initially and exhibit considerable decay (or flattening) before reaching the next row of bars. A very slight decrease in the successive values of maximum velocity is also evident.

The velocity profile upstream from each row exhibits the usual shape of a slightly retarded (decelerated) pipe flow. It also indicates that no flow separation occurred in the diverging portions of the test cell upstream of the first row of tubes. Crossflow effects on the pitot tube probably cause the measured velocities in the steep gradient regions near the edges of the jets to be somewhat higher than the actual speeds. On the other hand, velocities near the jet peaks should be much more accurate.

Wall pressure distributions for four mass flow rates (See Table I) are shown in Fig. 9. The wall pressures have been normalized with the plenum (or receiver) pressure,  $P_0$ . This latter pressure, it should be noted, is considerably larger than the local stagnation pressure.

Values of  $P_0$  may be obtained from Table I for the four runs. The number of rows of bars located between successive taps is also indicated in Fig. 9. It is evident that the wall pressure distributions were very nearly linear, as was postulated in the foregoing theoretical model. It should be noted that the last static tap was located between the seventh and eighth rows of bars so that the gas expansion loss which occurs downstream of the last row of tubes would be excluded, thus affording a better comparison with theory.

The dimensionless pressure gradient shown as a function of the mass flux in Fig. 10 increases with the flow rate, as would be expected. This information may be used to estimate pressure drops for other flow conditions with similar geometries.

In determining experimental values of the pressure drop coefficient,  $\zeta$ , it was found that equation (42) was somewhat undesirable because of its dependence upon density, this being difficult to infer from other measured quantities. However, a more tractable expression for  $\zeta$  in terms of easily accessible quantities is

$$\zeta = g_c \Delta P / n_0 u_0^2 = g_c \Delta P / n G u_0 \quad (46)$$

where  $u_0$  is the average velocity at the minimum area, and  $G$  is mass flux, also based on the minimum area.

Because velocity profiles were obtained just downstream of a row of bars, i.e., displaced downstream from the minimum area by a distance equal to one-half the bar diameter plus the clearance between the bar and the pitot tube (a total of 0.070 in.), it was necessary to calculate the average velocity,  $U_o$ , from the measured profiles. This calculation was based on a parabolic velocity distribution at the probe. The relation between  $U_o$  and the maximum jet velocity  $U_j$  (See Fig. 11) is

$$2b_o u_o = (2/3) U_j (2b_o + d)$$

or, for the J-5 cooler geometry,

$$u_o = 1.09 u_j$$

The ratio of theoretical to experimental values of  $\zeta$  is shown in Fig. 12. The upper curve incorporates the theoretical prediction of equation (46) which is valid for  $s/b_o = 7.23$ . It is observed that the theory tends to overestimate the pressure loss for three out of the four runs. Results of an analysis similar to that in Section 2.2, but including variable density, demonstrated that compressibility effects were indeed negligible, as has been assumed.

Further consideration of possible sources of error lead to an exploration of the effects of multiple bar diameters in the test model (See Fig. 8). The smaller-diameter bars near the wall result in a change in  $s/b_o$  from 7.23 to 6.23 for that region between the two sizes of bars. Furthermore, for the region between the smaller bars and the wall, the equivalent  $s/b_o$  is 3.15. The predicted value of  $\zeta$ , based on these smaller  $s/b_o$  values, decreased from an initial 0.180 to 0.156 and 0.079, respectively. An effective value of  $\zeta$  for the complete test section was approximated by prorating the three  $\zeta$  values on a cross sectional area basis\*. This yields the relation

$$\zeta_{\text{eff}} = \zeta_a \left( \frac{A_a}{A} \right) + \zeta_b \left( \frac{A_b}{A} \right) + \zeta_c \left( \frac{A_c}{A} \right) \quad (47)$$

$$= (0.180)(0.584) + (0.156)(0.270) + (0.079)(0.145) = 0.158$$

The effective  $\zeta$  was thus 14 per cent smaller than that given by

\*The wall shear stress was neglected after preliminary estimates confirmed that its contribution was indeed negligible.

equation (41). The resulting ratio of theoretical to experimental values of  $\zeta$  is shown as the lower curve of Fig. 12. It is seen that the maximum error between theory and experiment has been reduced from 33 to 18 percent.

Figure 13 shows a comparison of the present results with those of Abramovich (Ref. 22) and Pierson (Ref. 25) for in-line arrays of bars. The theoretical pressure loss coefficient is also shown. Moreover, in this figure are the G values for the present study and for Pierson's data. The corresponding information was not known for the Abramovich study. It is noted that the data of Pierson was obtained at a flow rate and pipe Reynolds number considerably lower than in the present study. This may account for a portion of the disagreement between the theory and measured values.

Based on these results, the theoretical value of 0.025 for the constant in the pressure loss coefficient is considered to be too large for the J-5 spray cooler geometry. Consequently, consistent with the concept given in equation (47) and the behavior noted in Fig. 12, the value of the constant will be taken as approximately 0.020. Thus the pressure loss coefficient is taken as

$$\zeta = 0.020 (s/b_o) \quad (48)$$

for the J-5 geometry, with  $b_o$  being the half spacing between the larger diameter spray bars. It should be emphasized that equation (48) is unique for the J-5 configuration (See Fig. 14); however, either of equations (48) or (44) will give a reasonable estimate of the pressure loss coefficient for spray bars arrayed in a typical in-line configuration.

### SECTION III APPROXIMATE ANALYSIS OF SPRAY COOLERS

#### 3.1 THE PROBLEM

The design problem can be stated as follows: given exhaust flow parameters at the inlet of the spray cooler section, cooling water parameters, and specified spray-bar configuration and duct geometry, determine the number of rows of spray bars required to cool the exhaust stream to a temperature level suitable for the subsequent compression process and predict the pressure drop which is incurred by flow through the spray bank. Moreover, it is desirable to minimize, if possible, the amount of water droplet carryover to the compressors. With a predictive model for spray-cooler design, parametric evaluations are then possible to suggest optimal operating conditions and design features.

Although large amounts of cooling water are sprayed into the cooler, only a fraction of the cooling water will augment the exhaust gas flow as steam and droplets. Indeed, with large values for the ratio of mass flow rate of injected water spray to exhaust gas flow rate (typically about 50:1), most of the injected water will fall out and flow along the bottom of the duct to drain sumps beyond the cooler section. Thus, the cross-sectional area of the duct occupied by the two phase flow will not be circular since the liquid will form only a thin film on the upper part of the duct surface and most of the water will fill the lower portion of the duct. This behavior is only qualitatively described because it will depend upon mass flow rates, duct geometry, and the configuration of drain sumps.

Thus, the phase distribution within the cooler section probably will be a combined form of annular mist flow and stratified wave flow, the dispensed droplet - exhaust gas flow being in the annular mist flow regime and the excess cooling water flow along the bottom of the duct being in the wave flow regime. Moreover, as mentioned in Section 1.1, the flow within the cooler section is not fully developed in any sense because of the small length-to-diameter ratio of the spray cooler and the complex nature of the two-phase flow, especially since the water is injected at each successive row of spray bars. Thermodynamic equilibrium between the phases flowing under these conditions probably does not exist, although it is reasonable to suppose the exhaust gas flow leaving the cooler section will be saturated with steam because of the large ratios of water-spray to exhaust-gas flow rates used. Furthermore, the entrained droplet flow is probably not in mechanical equilibrium

with the gas phase flow, the droplets being accelerated in typical operation of the J-5 spray cooler.

These features of the problem and the current state of knowledge about the simultaneous phenomena involved augur against a precise description or model for spray cooler performance. Thus, the description given here must necessarily be an oversimplification and it represents only a first attempt to obtain a model suitable for the design of spray coolers.

### 3.2 THE DESIGN MODEL

The model to be presented is comprised of solutions to the momentum and energy equations augmented by arbitrary assumptions and expressions for mass conservations. The energy equation is used to calculate the temperature of the exhaust flow leaving the cooler section, this temperature being the major process design criterion. The momentum equation is used to obtain the outlet pressure, with which the pressure drop through the cooler is calculable. The solution to the problem is complicated by the coupled nature of the momentum and energy equations and by the discrete conditions caused by the arrangement of successive rows of spray bars in the tube bank.

Although it is possible to write the energy, mass, and momentum conservation equations to describe the phenomena involved in the spray cooling process, the present state of knowledge for two phase flow requires that a number of simplifying assumptions be made if useful expressions are to be derived from the basic equations. The initial assumptions made in the model given here include the following: (1) ideal gas behavior is assumed for the steam and exhaust gas components (2) frictional losses at the duct wall are neglected (3) momentum losses incurred in the acceleration of the droplets to the exhaust flow velocity are neglected (4) momentum exchanges as droplets enter the liquid film or are entrained from the liquid surface are ignored.

The first assumption given above is probably not too severe because pressures are reasonably low and temperatures are high in much of the cooler section. The restrictions inherent in the assumed ideal behavior may, moreover, be alleviated by use of a better equation of state for the exhaust mixture. However, the added complexity seems unwarranted at this stage of the theoretical development. The neglect of frictional losses at the duct wall, taken as the second assumptions, is likewise probably reasonable. The major momentum effects will be those associated with tube drag and with the injected water spray. Furthermore, the frictional losses at the wall are difficult to estimate under the best of two-phase flow conditions, as was discussed in Section I; the flow conditions within

the spray cooler make such estimation even more formidable.

The third and fourth assumptions are less tenable than the former assumptions. There is obviously momentum exchange in terms of droplet drag as these particles are accelerated to the exhaust flow velocity. Furthermore, the problem is additionally complicated with mass transfer by condensation or evaporation of droplets. The momentum exchanges between the droplets and liquid film is even a more complex problem. The interfacial conditions at the liquid film surface are not amenable to any simple description. Much more detailed knowledge of these features of the flow must be gained before they can be treated realistically in a model, such as that presented here.

The extent to which the model is deficient for taking such assumptions depends upon the relative magnitudes of these effects which are ignored and those which are retained in the model. It is believed for the spray cooler problem that these neglected effects, although important, are not of major importance when compared to other momentum exchanges which are considered.

The analysis is based on the configuration and control volumes shown in Fig. 15, different control volumes being selected for the estimation of losses caused by tube drag and by other mechanisms. It is assumed that the inlet pressure  $P_0$ , inlet temperature  $T_0$ , mass flow rates of rocket exhaust and steam injected upstream from the spray cooler, and the rocket exhaust gas composition are known. The steam formed as a combustion product in the exhaust is added to the steam flow rate from the ejector to obtain the total steam flow rate entering the spray cooler. Moreover, any condensable components of the rocket exhaust (such as alumina in the case of solid propellants) are also subtracted from the exhaust gas flow, and the exhaust gas properties and flow rates are then calculated on the basis of the "noncondensable" exhaust flow. Thus, this "exhaust gas" flow rate  $W_{ex}$  is constant through the spray cooler.

The cooling water  $W_{1i}$  sprayed into a control volume may: 1) be entrained as droplet flow  $W_d$  with the combined exhaust and steam flow  $W_e$ , 2) be vaporized to augment the steam flow  $W_s$ , or 3) fall out to increase the liquid flow  $W_{1f}$ . The droplet flow entering the control volume may leave the volume as droplet flow, be vaporized and leave as steam, or fall into the liquid flow. The steam flow into the control volume will be assumed either to leave as steam or to condense out to increase the liquid flow (that is, condensation is assumed to occur only on the peripheral liquid film surface rather than on the droplets or to form additional droplets.) The liquid flow entering the control volume is assumed to leave the control volume in the same

manner; that is, the net transfer of water droplets between the liquid and the core flow is to the liquid surface. Moreover, drain sumps are assumed not to be located within the spray cooler section.

Mass balances written for the n-th control volume give

$$W_{\text{exn-1}} = W_{\text{exn}} = W_{\text{ex}} \quad (49)$$

for the exhaust gas flow (as defined above) and

$$W_{\text{lfn-1}} + W_{\text{sn-1}} + W_{\text{dn-1}} + W_{\text{li}} = W_{\text{lfn}} + W_{\text{sn}} + W_{\text{dn}} \quad (50)$$

for the water.

At this point in the analysis it is necessary to postulate that the cooling spray flow rate is sufficiently large that the entrained droplet flux will depend only upon the "carrying capacity" of the total exhaust stream. It is assumed for this purpose that the droplet flow rate is proportional to the total exhaust flow and may be expressed as

$$G_{\text{dn}} = \gamma_n (G_{\text{sn}} + G_{\text{exn}})$$

or

$$W_{\text{dn}} = \gamma_n (W_{\text{sn}} + W_{\text{exn}}) \quad (51)$$

which is a definition of  $\gamma_n$ , an "entrainment parameter". While such a definition of a droplet entrainment parameter might be considered prestidigitation, and while such a definition admittedly ignores all description of droplet entrainment mechanisms, the presumption of such a postulate may be almost ineluctable on a simple phenomenological basis, consistent with the assumption stated above.

Thus, the change in the liquid flow rate across the control volume can be expressed in terms of the injected spray flow rate, the steam flow rates, and the exhaust gas flow rate using equations (49), (50), and (51) to give

$$W_{\text{lfn}} - W_{\text{lfn-1}} = W_{\text{li}} - W_{\text{sn}} + W_{\text{sn-1}} - \gamma_n (W_{\text{sn}} + W_{\text{ex}}) + \gamma_{n-1} (W_{\text{sn-1}} + W_{\text{ex}}) \quad (52)$$

It will be convenient in the development of the engineering model for the prediction of pressure drop in spray coolers to consider separately that pressure loss caused by tube drag and that associated with other momentum losses. For typical operating condition, these two effects will normally oppose each other, the tube drag causing a pressure loss and the injected water spray being

sufficient to cause a pressure rise through the cooler section.

The momentum losses other than those caused by tube drag are expressed by a momentum balance written across the n-th control volume as

$$g_c \Delta P' = (W_{ex} + W_s + W_d)_n V_n - (W_{ex} + W_s + W_d)_{n-1} V_{n-1} - W_{li} V_{li} + W_{lfn} V_{lfn} - W_{lfn-1} V_{lfn-1} \quad (53)$$

in which the simplifying assumptions mentioned earlier pertaining to momentum losses have been taken. If it is assumed that the liquid flows along the duct wall at a constant velocity  $V_{lf}$ , and using equation (52), one can express equation (53) as

$$g_c \Delta P' = (1 + \gamma_n) (W_{ex} + W_{sn}) V_n - (1 + \gamma_{n-1}) (W_{ex} + W_{sn-1}) V_{n-1} - W_{li} V_{li} + \left[ W_{li} - W_{sn} + W_{sn-1} - \gamma_n (W_{ex} + W_{sn}) + \gamma_{n-1} (W_{ex} + W_{sn-1}) \right] V_{lf} \quad (54)$$

The pressure loss caused by tube bank drag is predicted using an analysis patterned after that by Abramovich (Ref. 22) and results of the work described in Section II. However, this analysis incorporates modifications to account for the two phase flow, whereas the Abramovich analysis applies only to single-phase flow over an array of tubes.

The modifications are based on the concept of the "homogeneous model" (see Section 1.5) in which it is assumed that the liquid droplets and exhaust gases flow as a homogeneous mixture with zero relative velocity between the phases. In this analysis, only that portion of the injected cooling water which forms steam and that which is entrained as droplet flow are taken with the exhaust gas flow to comprise a hypothetical mixture for the "core" flow, and only this flow is considered pertinent to the tube bank drag problem. The tube drag losses associated with the flow of the liquid film across the ends of the spray bars at the duct wall are ignored.

Thus, with use of equation (48) to express the pressure loss coefficient, the pressure drop per row of spray bars caused by tube drag is expressible as

$$\Delta P_i = \frac{0.020}{g_c} \left( \frac{s}{b_o} \right) \frac{G_{Tn-1}^2}{\rho_{en-1}} \quad (55)$$

in which  $G_T$  is the total combined exhaust and droplet flux and  $\rho_e$  is the combined exhaust density taken equal to  $\rho_{ex} + \rho_s$ . The total combined exhaust-droplet flux can, by use of equation (51), be written as

$$G_{Tn-1} = \frac{(1+\gamma_{n-1})(W_{ex} + W_{sn-1})}{A_m \alpha_{n-1}} \quad (56)$$

where  $\alpha$  is the void fraction and can be obtained, for example, from the empirical correlation of Yagi et al. (Ref. 26):

$$\alpha = \left[ 68 \left( \frac{W_1}{W_e} \right)^{0.88} \left( \frac{\rho_e}{\rho_1} \right)^{0.88} \left( \frac{1}{G_1} \right)^{0.6} \mu_1^{0.2} + 1 \right]^{-1} \quad (57)$$

As the mixture leaves the last row of tubes in the tube bank, there will be a terminal expansion which causes an additional pressure loss and, again following the Abramovich analysis, this is given by

$$\Delta P'' = \left[ 1 - \frac{2b_o}{L} \right]^2 \frac{G_{TN}^2}{g_c \rho_{eN}} \quad (58)$$

Equations (55), (56), and (58) are combined to give the pressure loss across the n-th control volume caused by the spray bar drag as

$$TD = \frac{0.020}{g_c} \left( \frac{s}{b_o} \right) \frac{(1+\gamma_{n-1})^2 (W_{ex} + W_{sn-1})^2}{\rho_{en-1} A_m^2 \alpha_{n-1}^2} + \left[ 1 - \frac{2b_o}{L} \right]^2 \frac{(1+\gamma_N)^2 (W_{ex} + W_{sN})^2}{g_c \rho_e A_m^2 \alpha_N^2} \quad (59)$$

The total pressure drop across the n-th control volume is then expressed as the sum,

$$P_n - P_{n-1} = -\Delta P' - TD$$

or

$$\begin{aligned}
P_n = & P_{n-1} - \frac{1}{g_c A} \left\{ (1+\gamma_n) (W_{ex} + W_{sn}) V_n - (1+\gamma_{n-1}) (W_{ex} + W_{sn-1}) V_{n-1} \right. \\
& \left. - W_{li} V_{li} + \left[ W_{li} - W_{sn} + W_{sn-1} - \gamma_n (W_{ex} + W_{sn}) + \gamma_{n-1} (W_{ex} + W_{sn-1}) \right] V_{lf} \right\} \\
& - \frac{0.020}{g_c} \left( \frac{s}{b_o} \right) \frac{(1+\gamma_{n-1})^2 (W_{ex} + W_{sn-1})^2}{\rho_{en-1} A_m^2 \alpha_{n-1}^2} \\
& - 1 - 2 \frac{b_o}{L} \frac{(1+\gamma_N)^2 (W_{ex} + W_{sN})^2}{g_c \rho_{eN} A_m^2 \alpha_N^2} \tag{60}
\end{aligned}$$

where the last term (the terminal expansion term) is included only if  $n=N$ , the last control volume. Equation (60) represents the form of the momentum equation to be used in the model.

Consider next an energy balance written for the  $n$ -th control volume which, under steady flow conditions, (a severe assumption), gives

$$\begin{aligned}
H_{li} = & (H_{sn} - H_{sn-1}) + (H_{dn} - H_{dn-1}) \\
& + (H_{exn} - H_{exn-1}) + (H_{lfn} - H_{lfn-1}) \tag{61}
\end{aligned}$$

in which:

$$H_{sn} - H_{sn-1} = W_{sn-1} \bar{C}_{ps} (T_n - T_{n-1}) + (W_{sn} - W_{sn-1}) h_{fg} \tag{62}$$

$$\begin{aligned}
H_{dn} - H_{dn-1} = & \gamma_{n-1} (W_{ex} + W_{sn-1}) \bar{C}_{pl} (T_n - T_{n-1}) \\
& + \left[ \gamma_n (W_{ex} + W_{sn}) - \gamma_{n-1} (W_{ex} + W_{sn-1}) \right] \bar{C}_{pl} (T_n - T_{cw}) \tag{63}
\end{aligned}$$

$$H_{exn} - H_{exn-1} = W_{ex} \bar{C}_{pex} (T_n - T_{n-1}) \tag{64}$$

$$H_{lfn} - H_{lfn-1} = (W_{lfn} - W_{lfn-1}) \bar{C}_{pl} (T_{lf} - T_{cw}) \tag{65}$$

$$H_{li} = W_{li} h_{li} \tag{66}$$

The superscript bars used above indicate mean values for the heat capacities over the indicated temperature ranges. In equation

(62) it has been assumed that the liquid droplet evaporation to form steam occurs at  $T_n$ ; this is consistent with another assumption that must subsequently be made. Moreover, in equation (65) the cooling water temperature rise for the liquid flowing along the duct wall has been taken to be constant, and the difference in liquid flow rates is obtained from the mass balance for the water, equation (52). Temperature equilibrium between the droplets and the combined exhaust and steam flow has been assumed (equation 63) for the two phase flow as it leaves the control volume.

If the heat capacity of the liquid is taken as a constant over the entire range from  $T_{n-1}$  to  $T_n$ , some simplification of equation (60) can be made, and this, when solved for  $T_n$  gives

$$\begin{aligned}
 T_n = & \left[ \left\{ W_{sn-1} \bar{c}_{ps} + \gamma_{n-1} (W_{ex} + W_{sn-1}) c_{pl} + W_{ex} \bar{c}_{pex} \right\} T_{n-1} \right. \\
 & + W_{li} h_{li} - (W_{sn} - W_{sn-1}) h_{fg} - (W_{lfn} - W_{lfn-1}) c_{pl} (T_{lf} - T_{cw}) \\
 & \left. + \left\{ \gamma_n (W_{ex} + W_{sn}) - \gamma_{n-1} (W_{ex} + W_{sn-1}) \right\} c_{pl} T_{cw} \right] / \left\{ W_{sn-1} \bar{c}_{ps} \right. \\
 & \left. + W_{ex} \bar{c}_{pex} + \gamma_n (W_{ex} + W_{sn}) c_{pl} \right\} \tag{67}
 \end{aligned}$$

Equations (52), (60), and (67) comprise the mathematical model for the design problem. The solution is iterative in nature and begins at the inlet of the spray cooler, considering first only one row of spray bars as the tube bank. If sufficient reduction of the exhaust temperature has not been achieved, a second row is added and the problem is continued. This procedure continues until the desired temperature has been reached at the outlet of the cooler, and the pressure drop across the cooler is determined.

In this computational procedure, it is presumed that the following information and system parameters are either known or specifiable:

$$A, A_m, S, b_o, L, W_{li}, \gamma, V_{li}$$

$$V_{lf}, T_{lf}, T_{cw}, C_{ps}, C_{pl}, C_{pex}, h_{li}$$

Furthermore, the following variables are assumed to be known at the inlet to the cooler section:  $W_{so}, W_{ex}, P_o,$  and  $T_o$  (recall that  $W_{so}$  includes the steam from both the ejector and from the combustion process, and that  $W_{ex}$  is the "noncondensable" exhaust gas flow rate).

Knowing these four quantities and the exhaust gas composition, one can obtain  $\rho_{eo}$  and  $V_o$  as follows:

$$\rho_{so} = \frac{y_{so} P_o}{R_{gs} T_o} \quad (68)$$

in which  $y_{so}$  is the mole fraction of steam:

$$\rho_{exo} = (1-y_{so}) P_o / R_{gex} T_o \quad (69)$$

$$\rho_{eo} = \rho_{so} + \rho_{exo} \quad (70)$$

and

$$V_o = \frac{W_{ex} + W_{so}}{\rho_{eo} A \alpha_o} \quad (71)$$

in which  $\alpha_o$  is unity (equation 57) since the flow at the inlet of the cooler is assumed to be only exhaust gas and steam.

Inspection of equations (52), (60), and (67) with  $n=1$  indicates the following quantities are yet unknown:  $T_1$ ,  $P_1$ ,  $W_{s1}$ ,  $V_1$ ,  $\rho_{e1}$ , and  $\alpha_1$ . However, if  $T_1$ ,  $P_1$ , and  $W_{s1}$  are found, then  $V_1$ ,  $\rho_{e1}$  and  $\alpha_1$  are readily calculable. Because equation (52) is used in equations (60) and (67), one is left with two equations (for  $T_n$  and  $P_n$ ), which are coupled in  $W_{sn}$ , and three unknowns  $T_n$ ,  $P_n$ , and  $W_{sn}$ . Thus a further assumption is necessary to obtain a solution to the problem, viz., that the relative humidity is unity for the combined exhaust flow as it leaves the control volume.

Thus, the following two-fold iterative scheme can be employed: Assume a value of  $T_1 = T_1^A$  and (for 100 per cent relative humidity) obtain the partial pressure of the steam  $P_{s1}^*$  from the water vapor pressure curve (or calculate it from a polynomial expression of the curve). The density is then calculated as

$$\rho_{s1} = P_{s1}^* / R_{gs} T_1^A \quad (72)$$

Next, assume a value of  $P_1 = P_1^A$  and obtain the exhaust gas density from

$$\rho_{ex1} = (P_1^A - P_{s1}^*) / R_{gex} T_1^A \quad (73)$$

The total density is then

$$\rho_{e1} = \rho_{s1} + \rho_{ex1} \quad (74)$$

The steam flow rate  $W_{s1}$  is calculated as

$$W_{s1} = \frac{W_{ex} R_{ex} P_{s1}^*}{(P_1^A - P_{s1}^*) R_{gs}} \quad (75)$$

and the velocity is

$$V_1 = \frac{W_{ex} + W_{s1}}{\rho_{e1} A \alpha_1} \quad (76)$$

where  $\alpha_1$  is calculated from equation (57).

At this point,  $\rho_{e1}$ ,  $\alpha_1$ ,  $V_1$ , and  $W_{s1}$  have been obtained based on  $T_1^A$  and  $P_1^A$ . Thus  $P_1$  can now be calculated from equation (60) with  $N=1$ , and  $P_1$  is compared with  $P_1^A$ . If  $P_1 \neq P_1^A$ , one must assume a different value for  $P_1^A$  and iterate these computations until  $P_1 = P_1^A$  to an acceptable agreement. When  $P_1$  has been obtained, equation (67) is used to calculate  $T_1$ , and this value is compared with  $T_1^A$ . The computation is then iterated on  $T_1$  (which necessarily involves iteration on  $P_1$ ) until  $T_1$  is known to acceptable accuracy.

The calculated value of  $T_1$  is then compared to the design temperature specified at the outlet of the cooler section. If the exhaust temperature is too high, the terminal expansion loss term,

$$1 - \left[ \frac{2b_o}{L} \right]^2 \frac{(1 + v_N)^2 (W_{ex} + W_N)^2}{g_c \rho_{eN}^A m^2 \alpha_N^2} \quad (77)$$

is computed and, if significant in magnitude, this term must be deleted from equation (60), for  $N=1$  and  $T_1$  and  $P_1$  re-computed before a second row of spray bars is added to the tube bank and the problem solved for  $N=2$ . In practice, one would probably not include this terminal expansion loss term until several rows of spray bars had been included and the calculated temperature approaches the specified design temperature at the outlet of the cooler section.

### 3.3 EVALUATION OF THE MODEL

Although development and refinement of the model is continuing, certain features of the model have been assessed using limited performance data available for the spray cooler in the J-5 Facility at AEDC. These data are abstracted and given in Table III. The rocket exhaust gas composition given in Table IV is taken as typical for the firings which gave the pressure drop data given in Table III. This rocket exhaust analysis was used to obtain the composition given in Table V for the noncondensable exhaust gas, in this case the rocket exhaust gas minus the steam and minus the alumina, which condenses out of the gas phase at about 5850°R and solidifies at about 4200°R. The initial exhaust temperature is approximately 6600°R.

The J-5 cooler configuration (see Fig. 14) includes eight rows of spray bars, only the first seven of which were operative when the data given in Table III were obtained. Dimensions pertinent to this analysis are also indicated in the figure.

A momentum equation modified from equation (60) to account for the unused last row of spray bars was used with the J-5 spray cooler specifications and firing data to test for consistency between predicted pressure drop and the measured values. Moreover, some knowledge of the behavior of the droplet entrainment parameter  $\gamma$  used to specify the water droplet flow rate was obtained.

An iterative procedure was used to obtain calculated values of the pressure drop versus assumed values of  $\gamma$  parametric in exhaust temperature at the inlet to the spray cooler. By specifying inlet temperature and knowing the inlet pressure and flow rate from data given in Table III, one can evaluate the quantities, such as exhaust density and velocity, needed in the computations. Similarly, knowing the outlet temperature from Table III and using an estimated pressure drop, one can calculate these same quantities at the outlet of the cooler.

At this point, a "stepped" distribution based on the number of rows of spray bars was assumed for these quantities (viz.: density, liquid film flow rate, droplet flow rate, velocity, and the combined exhaust flow rate) taking account that the last row of spray bars was inoperative during the firings noted in Table III. The parameter  $\gamma$  was also taken to be a stepped function between the inlet and outlet of the cooler as

$$\gamma_n = \frac{n}{N} \gamma_N \quad n = 1, 2, \dots, N \quad (78)$$

in which  $n$  denotes the  $n$ -th control volume and  $N = 7$  in this case;

that is,  $\gamma_7$  equals  $\gamma_8$  because the last row of spray bars was not used, although the tube drag and terminal expansion losses associated with the last row were included in the computations.

To facilitate these computations, a polynomial fit was made to the water vapor pressure curve over a range of saturation pressures from 0.75 to 7.0 psia. This expression,

$$T_s^* = 0.4811P_s^{*3} - 7.000P_s^{*2} + 41.97P_s^* + 66.29^{\circ}\text{F} \quad (79)$$

agrees to within one percent with the values determined experimentally over the indicated pressure range.

The calculations were iterated on the estimated pressure drop until the calculated and estimated values agreed. A ratio of the calculated pressure drop to the measured pressure drop listed in Table III was then computed. Figures 16 through 27 show this ratio plotted against the parameter  $\gamma_N$  parametric in values of exhaust inlet temperature. The data line designation in the figure captions refers to the corresponding line in Table III.

In the computations summarized by Fig. 16 through 27, parameters other than geometric and thermodynamic constants were taken as:

- 1) cooling water supplied to each row  
of spray bars.....10,000 gpm
- 2) average velocity of spray from nozzles,..... 200 fps
- 3) average velocity of liquid film..... 20 fps

The results for unit value of the pressure drop ratio and an inlet temperature of 3000 R suggest that the droplet entrainment parameter varies between three and four based on these test firings. The exceptional cases found in data lines 4 and 14 (Fig. 16 and 25) may reflect measurement errors in the observed pressure drops and/or outlet temperatures given in Table III. The pressure drop recorded in data line 14 appears to be too small when compared with similar firing data given in lines 15 and 16, for example. In cases when the reported pressure is low, the  $\gamma$  value corresponding to a unit value of the ratio (calculated pressure drop equal to experimental pressure drop) will be high. This is necessarily so because more droplet entrainment is required to give a pressure rise sufficient to offset more of the tube drag loss; thus, a higher  $\gamma$  value is obtained. The reported outlet temperature in data line 4 is low compared to similar firings for which all other data except outlet temperature are comparable to line 4.

A tentative correlation given as Fig. 28 is proposed to estimate values of the droplet entrainment parameter as a function of a correlating parameter which is effectively the energy loss associated with the flow divided by the mass flow rate of the exhaust stream. This correlation was made for unit values of the pressure drop ratio and with an exhaust inlet temperature of 3500°R. Again, and for the same reasons noted above, the results computed from data in lines 4 and 14 of Table III fall away from the pattern of the other points. These two points were thus ignored in obtaining the  $\gamma$  correlation. The scatter noted in the data in Fig. 28 could result from inadequacies of the proposed correlation and/or errors in the data reported in Table III. While this correlation does give some means of estimating the liquid droplet carryover from the spray cooler chamber, it does not obviate the need for a much more fundamental knowledge of liquid droplet entrainment processes to yield improved design of spray coolers.

The correlation for the droplet entrainment parameter could be used to specify those values needed in the computational procedure outlined earlier for the design model. This would necessarily introduce a third level of iteration into the computational scheme because assumed values of the correlating parameter used to obtain a  $\gamma$  value would subsequently need to be verified with a computed value of the correlating parameter.

To assess the influence of certain quantities within the model upon the predicted pressure drop, the data in line 13 were used as a basis to evaluate parametrically the effects of changes in the cooling water flow rate, droplet spray discharge velocity, liquid film velocity, and different values of the constant associated with the pressure loss coefficient. Results of these studies are presented in Fig. 29 through 32. With the exception of the case for variation in the cooling water flow rate (which is overwhelming in all cases), there is a significant change in the  $\gamma$  value corresponding to a unit value of the pressure drop ratio. Of these parameters, the liquid film flow rate is known with the least precision.

This evaluation of the momentum equation demonstrates that the approach taken in the design model is consistent with the experimental data available for spray cooler performance. However, these tests have involved only a portion of the total design model, and the further development of this work is being continued by The University of Texas.

#### SECTION IV CONCLUSIONS AND RECOMMENDATIONS

It can be concluded from the present investigation that the current state of knowledge of two-phase flow processes does not permit the development of a highly sophisticated, theoretical flow model for spray coolers. At best one must resort to a phenomenological approach with empirically based constants. However, it has been demonstrated that this technique does permit one to make estimates of cooler performance, although much additional work is needed.

This state of affairs therefore strongly suggests that, if further insight into the physical mechanisms of cooler flows is to be attained, a comprehensive and systematic experimentation program is required. Because spray coolers form a significant component of any rocket testing facility, it is obvious that AEDC would obtain benefit from the results of such a program, especially if it is carried out in conjunction with the normal testing activities of the center. In this way a considerable body of data can be accumulated in a relatively short time while avoiding any difficulties of exhaust gas simulation and modeling. Should such an on-site spray cooler development program be contemplated, there are a number of considerations which suggest themselves.

Because scaling laws for two-phase flow are not well developed, it is desirable that the instrumented test cooler be as large as possible. Short of running tests in a full-size device, it is believed that the test cooler should be at least one-fifth to one-fourth full size. It might be possible to arrange a duct-with-cooler of this size in parallel with the primary exhaust ducting.

The embryonic state of measurement techniques with which to study two-phase flow phenomena causes experimental difficulties. However, even the simplified approach presented in this report could be refined with only the availability of additional pressure and temperature measurements and a more complete inventory of the liquid flows. At present it appears that the entrained droplet flow rate within the spray cooler is obtainable only as the difference between the cooling water supplied and that removed through the drain sumps; proper account being taken for that water which is vaporized to add steam to the exhaust flow. Thermodynamic properties and flow rates of the exhaust flow into the cooler section must also be known.

Within the overall operational objectives of minimizing pressure loss and droplet carryover, while maximizing temperature drop,

some additional insight could be obtained by variation of the injected spray flow rate. This could be done during the normal course of operations or through computer simulation of the spray cooler performance using the model presented here. This latter approach is being continued in work at The University of Texas. Because the geometry of the spray bar configuration is important and, in many cases, difficult to treat analytically, the tube drag effects for other than the simple configurations will probably be best evaluated through experimental investigations. Even cold-flow pressure loss measurements would be useful in this part of the work.

The model presented here represents only a first step toward the improved design of spray coolers for rocket test facilities. The nature of the problem is entirely complex and the need is for a much improved understanding of two-phase flows from a fundamental standpoint. With such knowledge as will be gained in the future, models such as that presented here can be refined and extended to describe more fully the performance of spray cooler systems.

## REFERENCES

1. Dukler, A. E. and Wicks, M., "Gas-Liquid Flow in Conduits," in Modern Chemical Engineering, Vol. 1, Physical Operations, edited by Andreas Acrivos. Reinhold Publishing Company, 1963.
2. Gouse, S. W., "An Introduction to Two-Phase Gas-Liquid Flow," MIT Engineering Projects Laboratory Report No. DSR 8734-3, June, 1964, AD 603 659.
3. Charvonia, D. A., "A Review of the Published Literature Pertaining to the Annular, Two-Phase Flow of Liquid and Gaseous Media in a Pipe," Purdue University Technical Report Pur-32-R, December, 1958. AD 208 040.
4. Gresham, W. A., Foster, P. A., and Kyle, R. J., "Review of the Literature on Two-Phase (Gas-Liquid) Fluid Flow in Pipes," Part 1, WADC Technical Report 55-422, June 1955. AD 95 752.
5. Kutateladze, S. S. and Styrikovich, M. A., "Hydraulics of Gas-Liquid Systems," Gosudarstvennoye Energeticheskoye Izdatel'stvo, Moscow, 1958. AD 257 824 (Translation).
6. Govier, G. W., "Developments in the Understanding of the Vertical Flow of Two Fluid Phases," Canadian Journal of Chemical Engineering, Vol. 43, p. 3, February, 1965.
7. Gouse, S. W., "An Index to the Two-Phase Flow Literature," (in three parts), MIT Engineering Projects Laboratory Report Nos. DSR 8734-1, May, 1963 (AD 411 512); DSR 8734-4, September, 1964 (AD 607 180); DSR 8734-6, January, 1966 (AD 630 295).
8. Kepple, R. R. and Tung, T. V., "Two-Phase (Gas-Liquid) System: Heat Transfer and Hydraulics, An Annotated Bibliography," Argonne National Laboratory, July, 1963, ANL-6734.
9. "The Penn State Bibliography on Sprays," Second Edition, The Texas Company, 1953. AD 30 810.
10. Putnam, A. A. et al., "Injection and Combustion of Liquid Fuels," Battelle Memorial Institute, March 1957. AD 118 142.
11. Knowles, C. R., Silberberg, I. H. and Brown, K. E. "The Effect of Flow Patterns on Pressure Loss in Multiphase, Horizontal Flow," Texas Petroleum Research Committee, University Division, Report No. UT 65-3, December, 1965.

12. Baker, O., "Designing For Simultaneous Flow of Oil and Gas," The Oil and Gas Journal, p. 185, July 26, 1954.
13. Hsu, Y. Y., Simon, F. F. and Graham, R. W., "Application of Hot Wire Anemometry for Two-Phase Flow Measurements such as Void Fraction and Slip Velocity," ASME Multi-Phase Flow Symposium, November, 1963.
14. Magiros, P. G., and Dukler, A. E., "Entrainment and Pressure Drop in Concurrent Gas-Liquid Flow, II. Liquid Property and Momentum Effects, " in Developments in Mechanics, Vol. 1, edited by Lay, J. E. and Malvern, L. E., p. 532, Plenum Press, 1961.
15. Wicks, M., and Dukler, A. E., "Entrainment and Pressure Drop in Concurrent Gas-Liquid Flow: 1. Air-Water in Horizontal Flow," AIChE Journal, Vol. 6, No. 3, p. 463, September, 1960.
16. Dukler, A. E., Wicks, M., and Cleveland, R. G., "Frictional Pressure Drop in Two-Phase Flow: B. An Approach Through Similarity Analysis," AIChE Journal, Vol. 10, No. 1, p. 44, January, 1964.
17. Lockhart, R. and Martinelli, R. C., "Proposed Correlation for Data for Isothermal Two-Phase, Two Component Flow in Pipes," Chemical Engineering Progress, Vol. 45, No. 1, p. 39, January, 1949.
18. Levy, S., "Theory of Pressure Drop and Heat Transfer for Annular Steady State Two-Phase Two-Component Flow in Pipes," Proceedings of the Second Midwestern Conference on Fluid Mechanics, p. 337, 1952.
19. Levy, S., "Prediction of Two-Phase Pressure Drop and Density Distribution From Mixing Length Theory," Journal of Heat Transfer, Transactions of ASME, Series C, Vol. 85, p. 137, May, 1963.
20. Jayner, U.T., and Palmer, C. B., "An Experiment Survey of Flow Across Banks of Elliptical and Pointed Tubes," NACA Wartime Report, January, 1943.
21. Brevoort, M. J., and Tefford, A. N., "An Experimental Investigation of Flow Through Tube Banks," NACA Wartime Report, March 1942.
22. Abramovich, G. N., "The Theory of Turbulent Jets," The MIT Press, Cambridge, Mass., 1963.

23. Jones, J. W., "Experimental and Analytical Investigation of Flow Across Inline Tube Bank Arrays," MS Thesis, The University of Texas, January, 1968.
24. Schlichting, H., "Boundary Layer Theory," Fourth Edition, McGraw-Hill Book Company, New York, 1960.
25. Pierson, O.L., "Experimental Investigation of the Influence of Tube Arrangement on Convection Heat Transfer and Flow Resistance in Cross Flow of Gases Over Tube Banks," Transactions of ASME, Vol. 59, 1937, p. 563.
26. Yagi, S., Shirad, T., and Sasaki, T., "Studies on Vertical Pipe Reaction (I). Flow Pattern and Holdup in Gas-Liquid Two Phase Flow Through Vertical Pipe", Chem. Engr. (Japan), Vol. 15, 1957, p. 317.

**APPENDIXES**  
**I. TABLES**  
**II. ILLUSTRATIONS**

TABLE I  
VALUES OF EXPONENTS  $m$ ,  $n$ , AND CONSTANTS  $C_L$  AND  $C_G$  FOR VARIOUS  
LOCKHART-MARTINELLI COMBINATIONS OF VISCOUS AND TURBULENT FLOWS

---

<u>Flow Types</u>	<u>t-t</u>	<u>v-t</u>	<u>t-v</u>	<u>v-v</u>
$n$	0.2	1.0	0.2	1.0
$m$	0.2	0.2	1.0	1.0
$C_L$	0.046*	16.	0.046*	16.
$C_G$	0.046*	0.046*	16.	16.
$(Re)_{\text{liquid}}$	>2000	<1000	>2000	<1000
$(Re)_{\text{gas}}$	>2000	>2000	<1000	<1000

---

\*For smooth pipes

---

**TABLE II**  
**TEST CONDITIONS USED IN TUBE BANK PRESSURE DROP MEASUREMENTS**

---



---

Run	<u>G (note 1)</u> <u>lbm/sec ft<sup>2</sup></u>	<u><math>\dot{m}</math></u> <u>lbm/sec</u>	<u>Re</u> <u>(note 2)</u>	<u>P<sub>o</sub> (abs)</u> <u>in.Hg</u>
1	32.4	.405	$4.56 \times 10^6$	59.8
2	44.1	.550	$6.20 \times 10^6$	81.0
3	63.3	.788	$8.91 \times 10^6$	111.6
4	79.8	.995	$11.20 \times 10^6$	138.1

---

Note: 1. G based on minimum flow area between bars  
 2. Re based on test section diameter

---

TABLE III  
PRESSURE DROP DATA FROM J-5 SPRAY COOLER

Data Line	Firing Number	Rocket Exhaust Flow lbm/sec	Steam Ejector Flow lbm/sec	Inlet Pressure psia	Pressure Drop psi	Outlet Temperature °F
4	3402-04	250	101	4.00	-1.40	128
5	0407-01	250	89	6.10	-2.00	143
6	0421-01	250	115	5.70	-1.80	141
8	0421-03	237	169	5.10	-1.80	133
9	0421-04	226	100	4.60	-1.70	128
10	0421-05	250	87	6.10	-1.80	143
11	0421-06	250	135	6.60	-1.80	148
12	0447-01	246	326	7.00	-1.90	153
13	0447-02	246	100	6.00	-2.20	140
14	1528-01	30	133	1.48	-0.20	102
15	1528-02	30	150	1.50	-0.35	103
16	1528-03	30	156	1.40	-0.30	100

Note: Cooling water flow was approximately 70,000 gpm.

TABLE IV  
TYPICAL SOLID FUEL ROCKET EXHAUST COMPOSITION\*

---

<u>Component</u>	<u>Weight Fraction</u>	<u>Mole Fraction</u>
H <sub>2</sub>	0.0170	0.2472
H <sub>2</sub> O	0.0487	0.0793
CO	0.3586	0.3753
CO <sub>2</sub>	0.0319	0.0213
N <sub>2</sub>	0.1370	0.1434
Al <sub>2</sub> O <sub>3</sub>	0.3749	0.1078
HCl	0.0315	0.0254
	<hr style="width: 50%; margin: 0 auto;"/>	<hr style="width: 50%; margin: 0 auto;"/>
	0.9996	0.9997

---

Molecular weight = 29.31

Specific gas constant = 52.68

\*At temperature  $\approx 6600^{\circ}\text{R}$

---

TABLE V  
 "NONCONDENSABLE" ROCKET EXHAUST GAS ANALYSIS\*

---



---

<u>Component</u>	<u>Weight Fraction</u>	<u>Mole Fraction</u>
H <sub>2</sub>	0.0295	0.3041
CO	0.6224	0.4618
CO <sub>2</sub>	0.0554	0.0262
N <sub>2</sub>	0.2377	0.1764
HCl	0.0547	0.0312
	<u>0.9997</u>	<u>0.9997</u>

Molecular weight = 20.78

Specific Gas constant = 74.30

\*Based on composition given in Table IV without H<sub>2</sub>O and Al<sub>2</sub>O<sub>3</sub>.

---

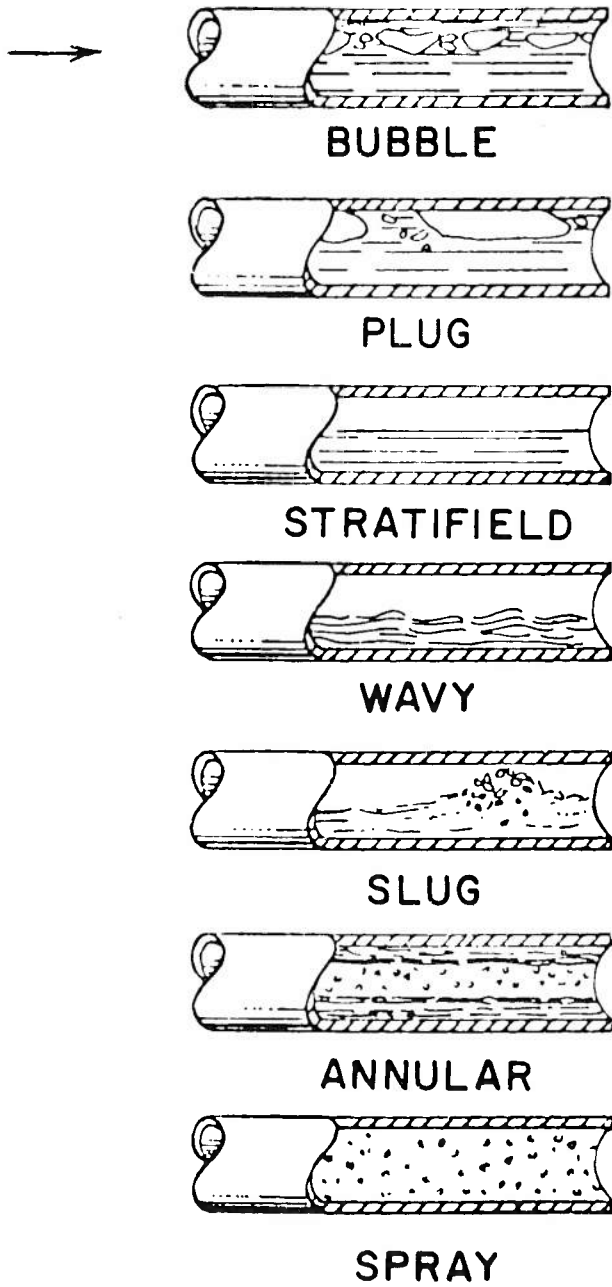


Fig. 1 Schematic Drawings of Flow Patterns in Horizontal Adiabatic Two-Phase Flow

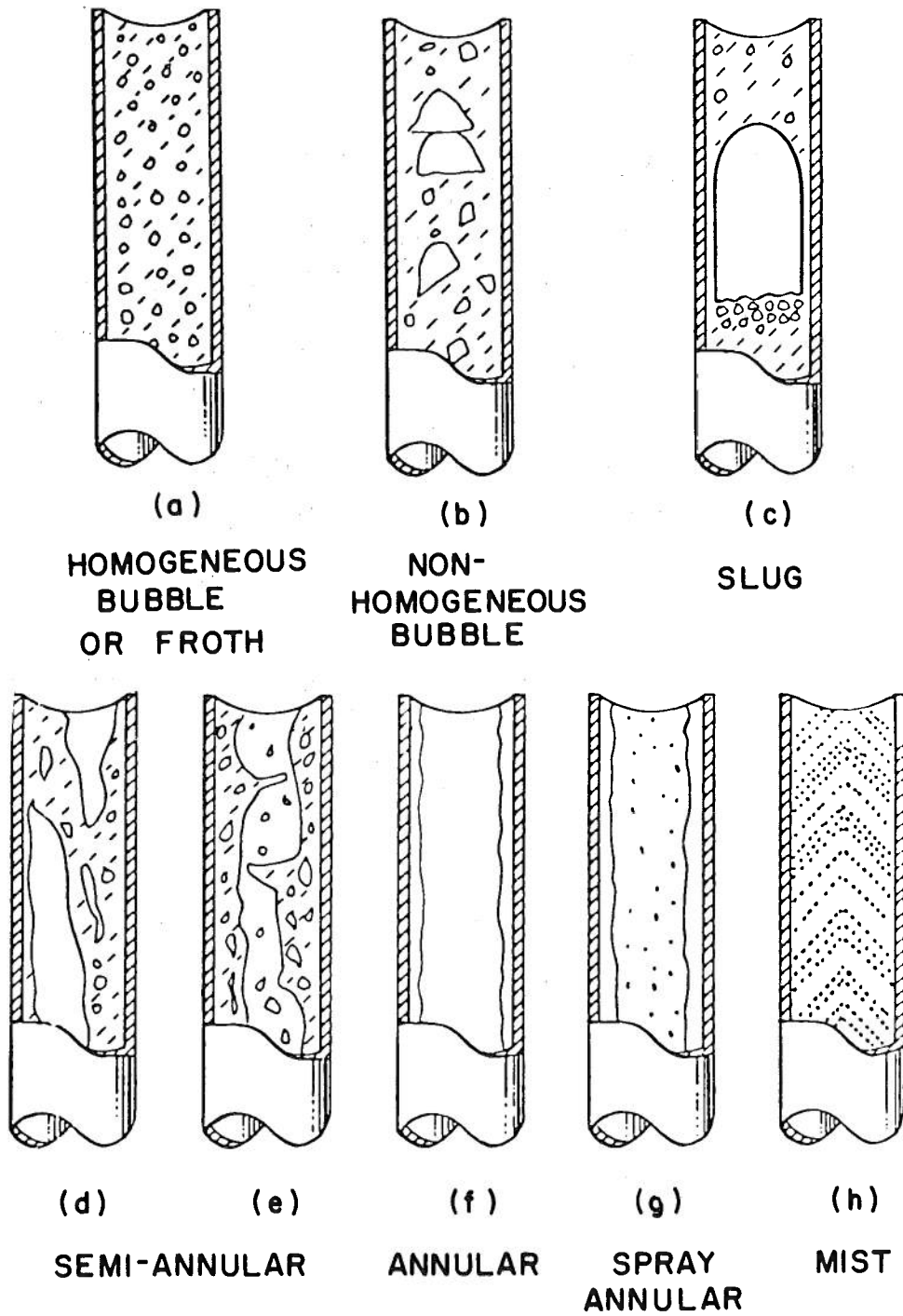
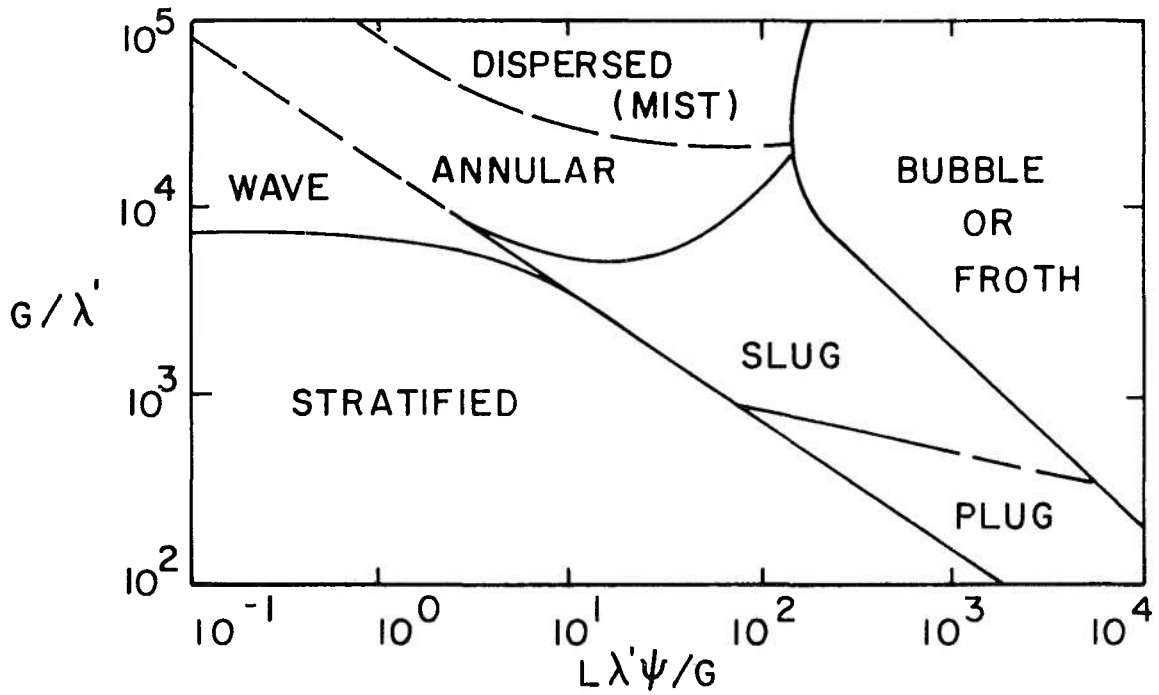


Fig. 2 Schematic Drawings of Flow Patterns in Adiabatic Two-Phase Vertical Upflow



$L$  = mass flux of liquid phase

$G$  = mass flux of gas phase

$$\lambda' \sim (\rho_G \rho_L)^{1/2}$$

$$\psi \sim \mu_L^{1/3} / \nu \rho_L^{2/3}$$

$\nu$  = surface tension

Fig. 3 Baker Flow Pattern Chart for Two-Phase Flow

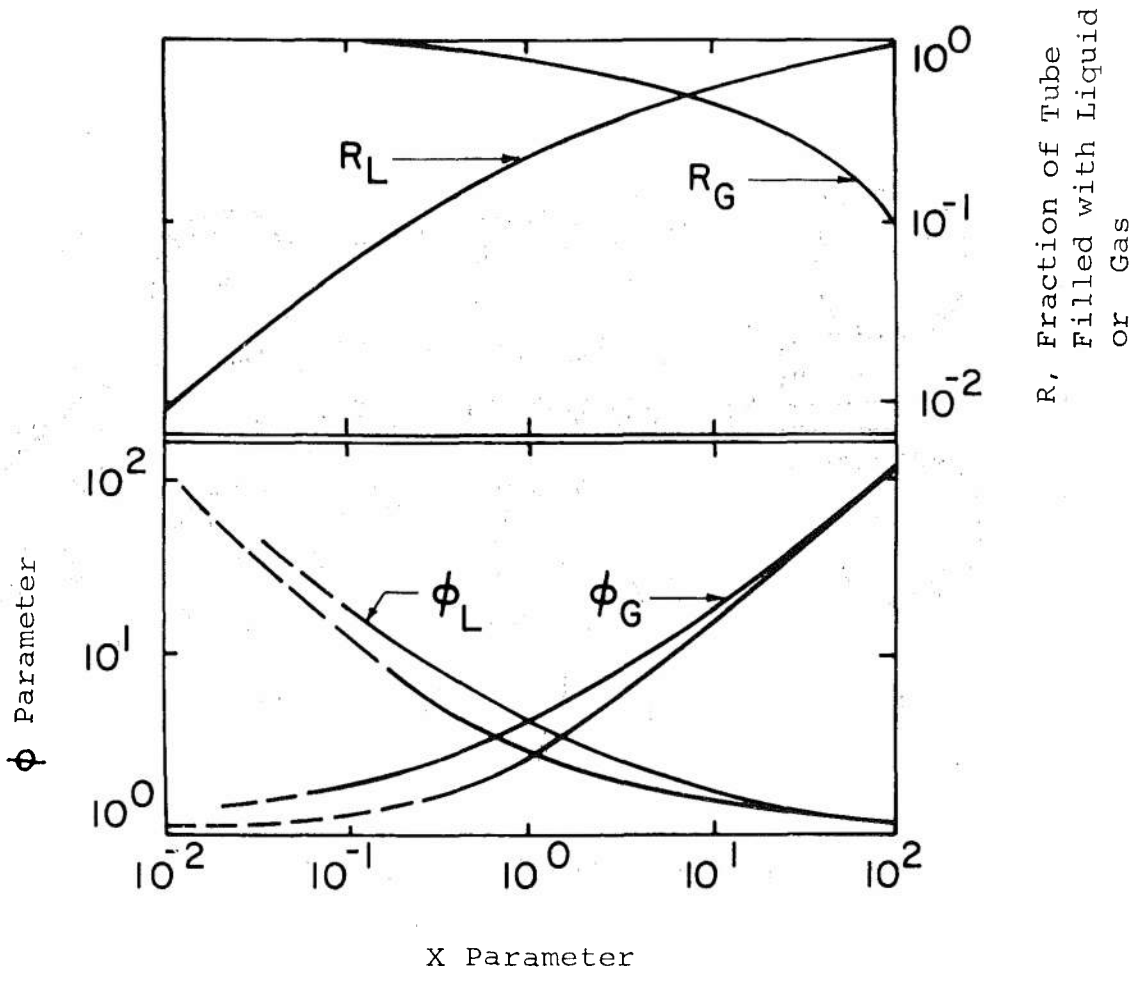


Fig. 4 Results of Lockhart-Martinelli Correlation

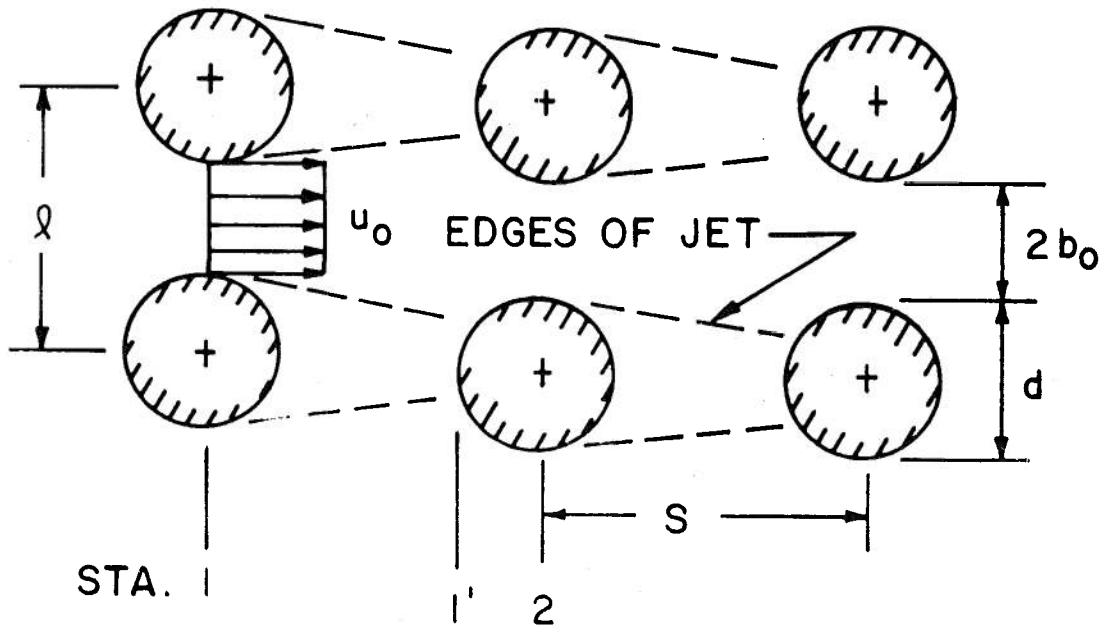


Fig. 5 Schematic of Flow Pattern in Tube Bank

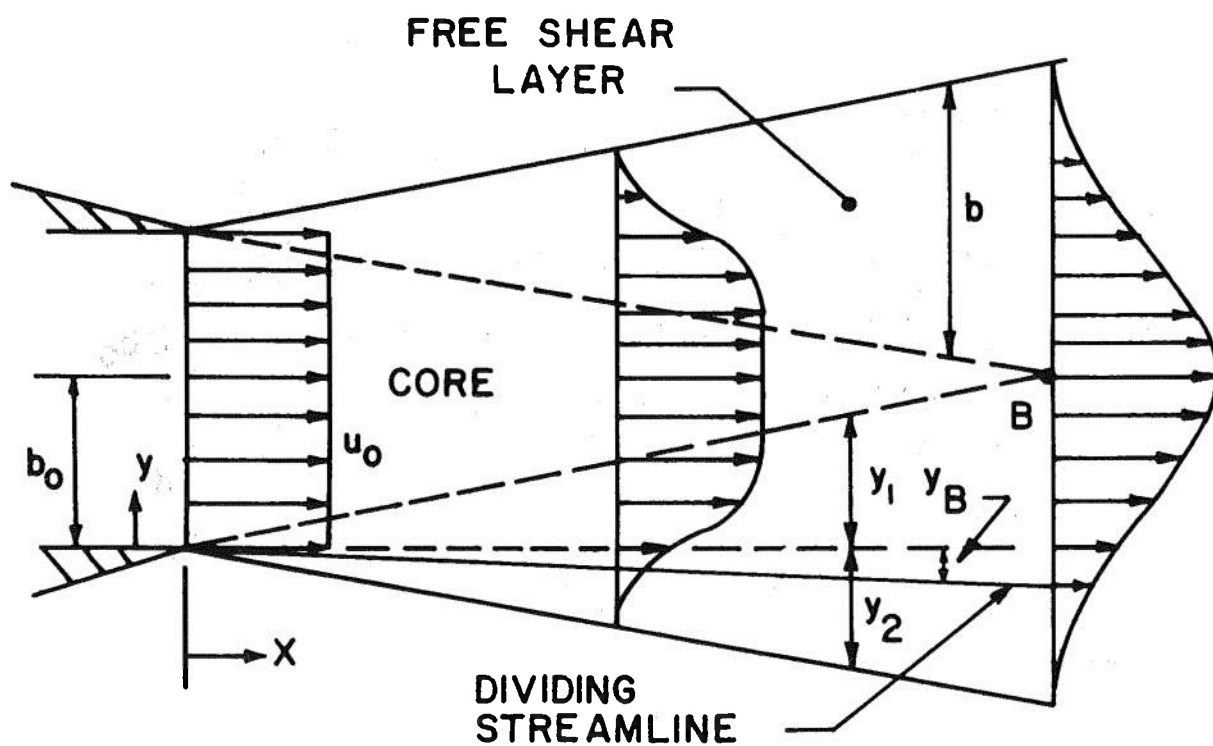
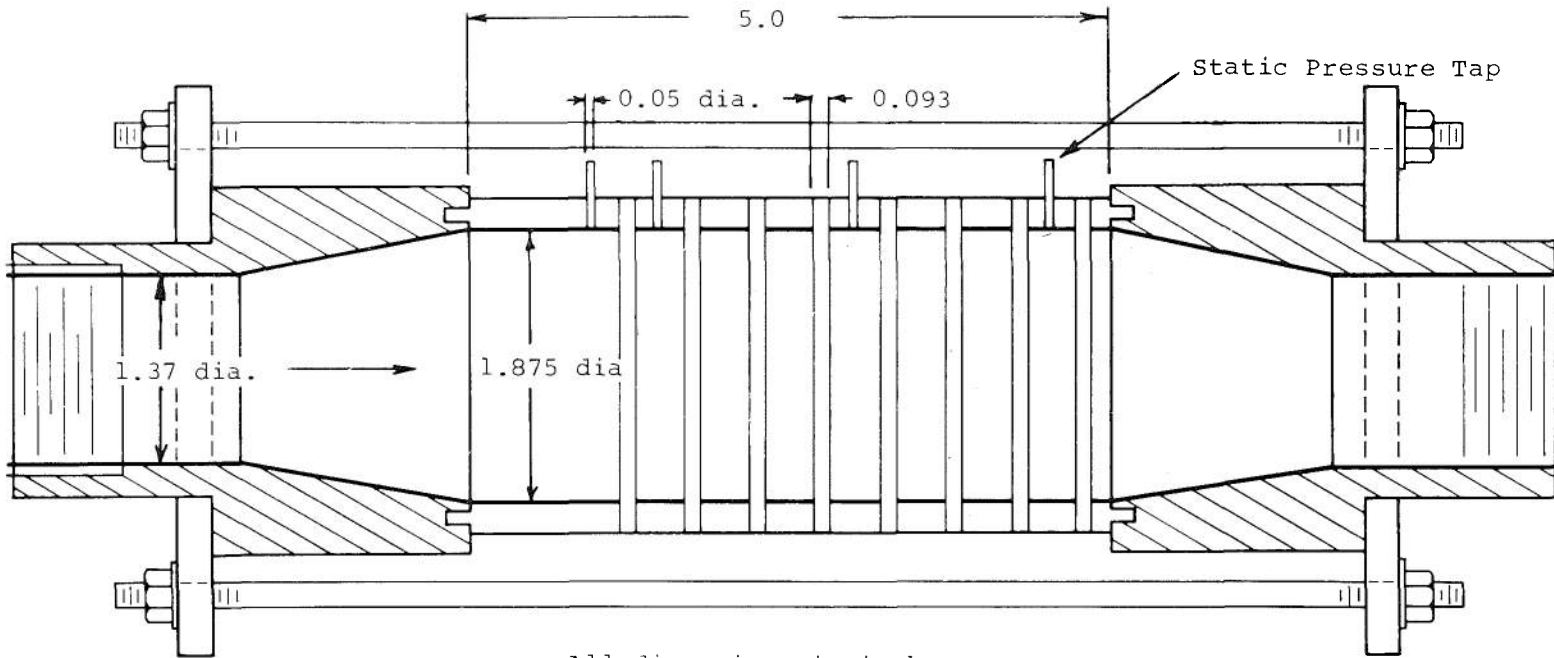


Fig. 6 Geometry of Initial Region of Free Jet, Showing Typical Velocity Profiles



All dimensions in inches

Fig. 7 Cross-Sectional View of Test Section for Air Flow Experiments

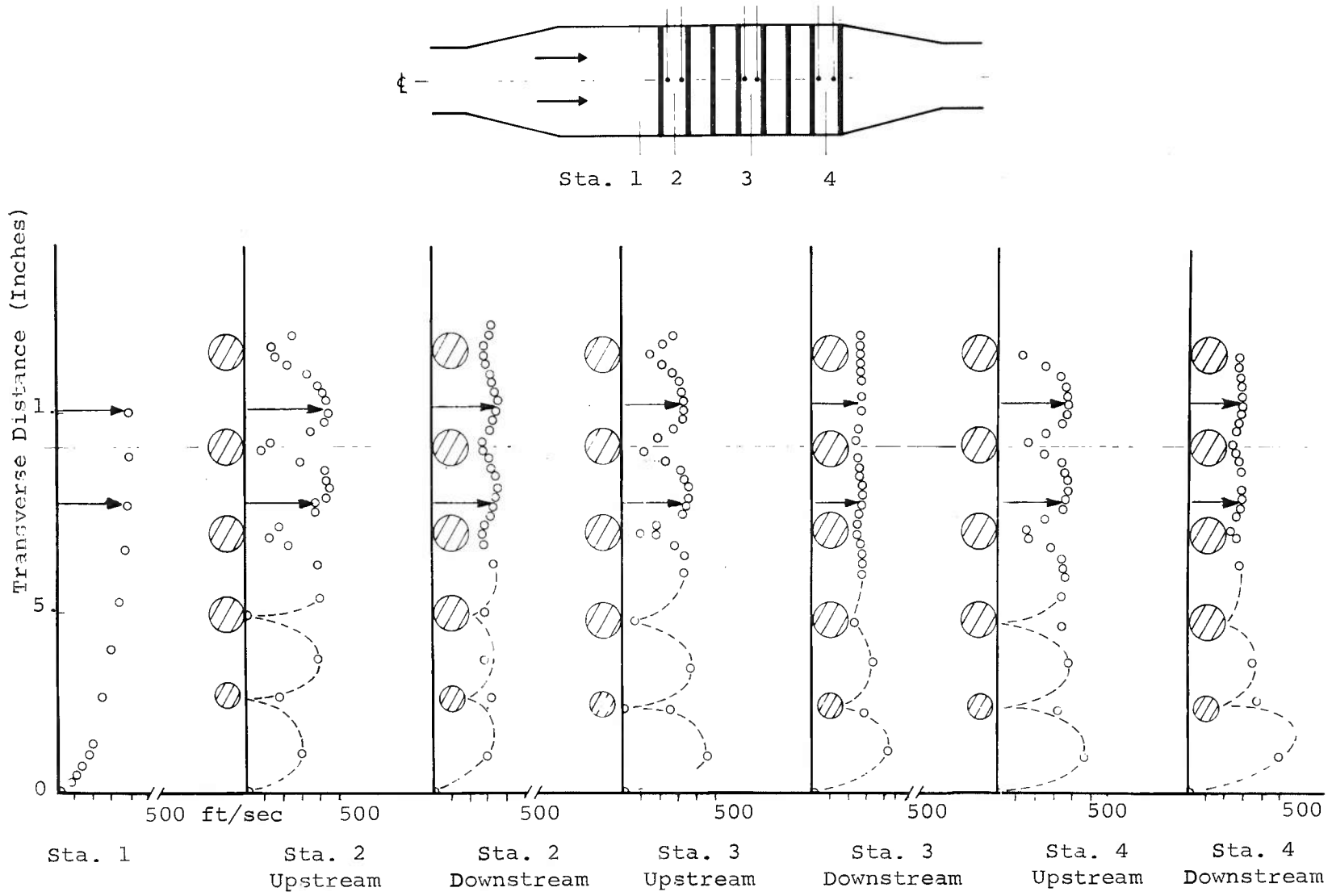


Fig. 8 Typical Velocity Profiles at Various Stations in Tube Bank

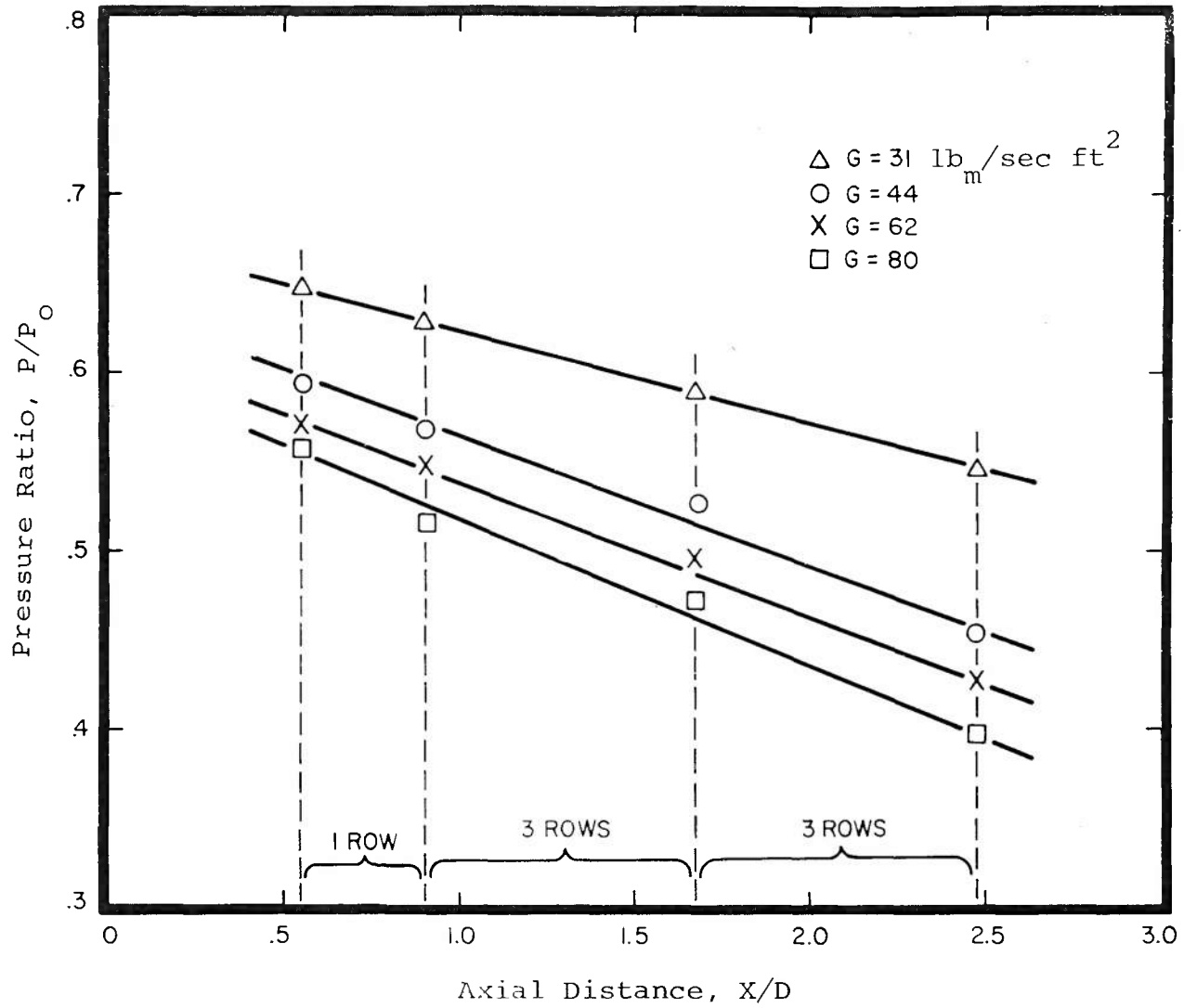


Fig. 9 Wall Static Pressure Distributions

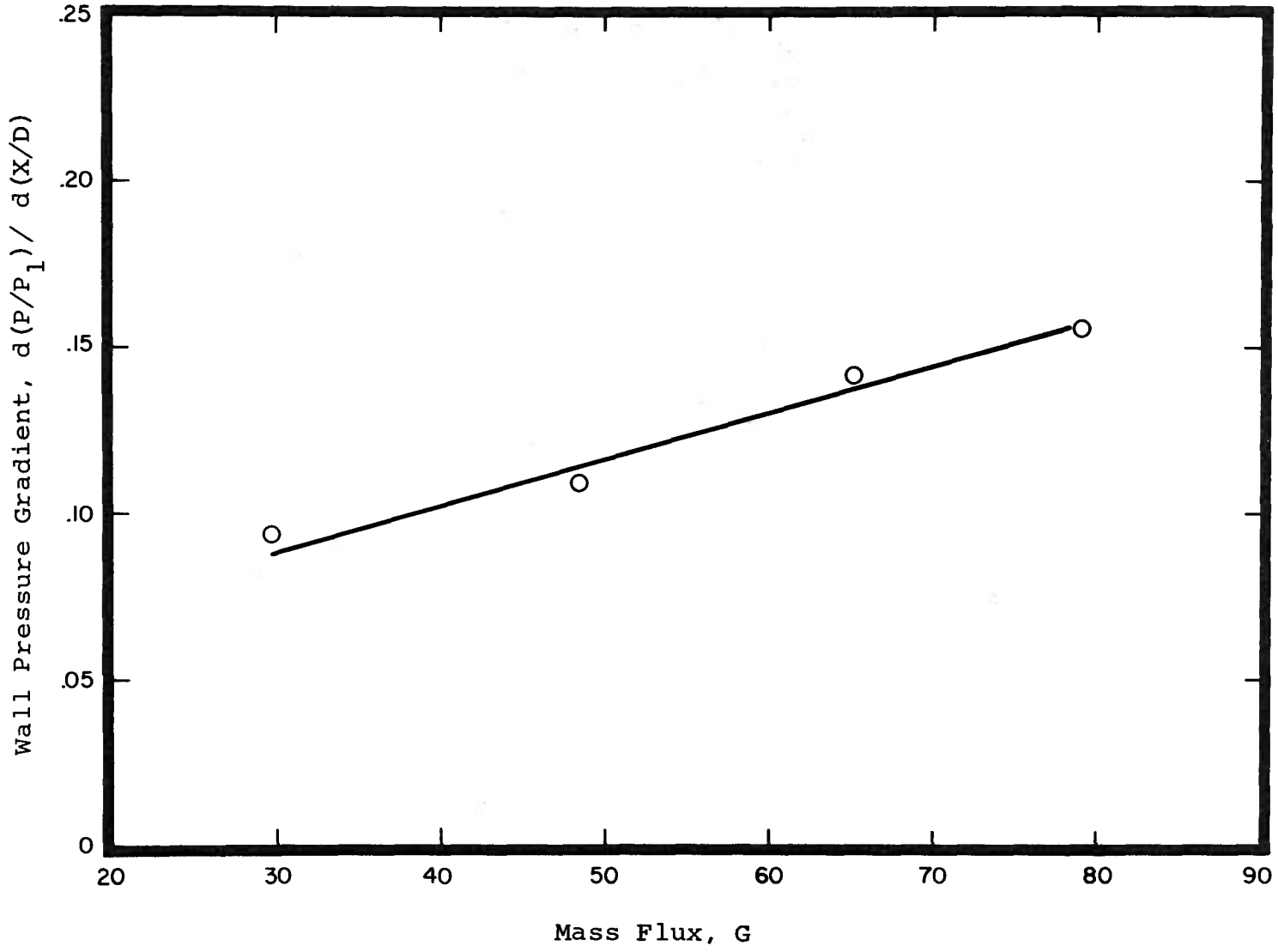


Fig. 10 Generalized Wall Static Pressure Gradient as a Function of the Mass Flux

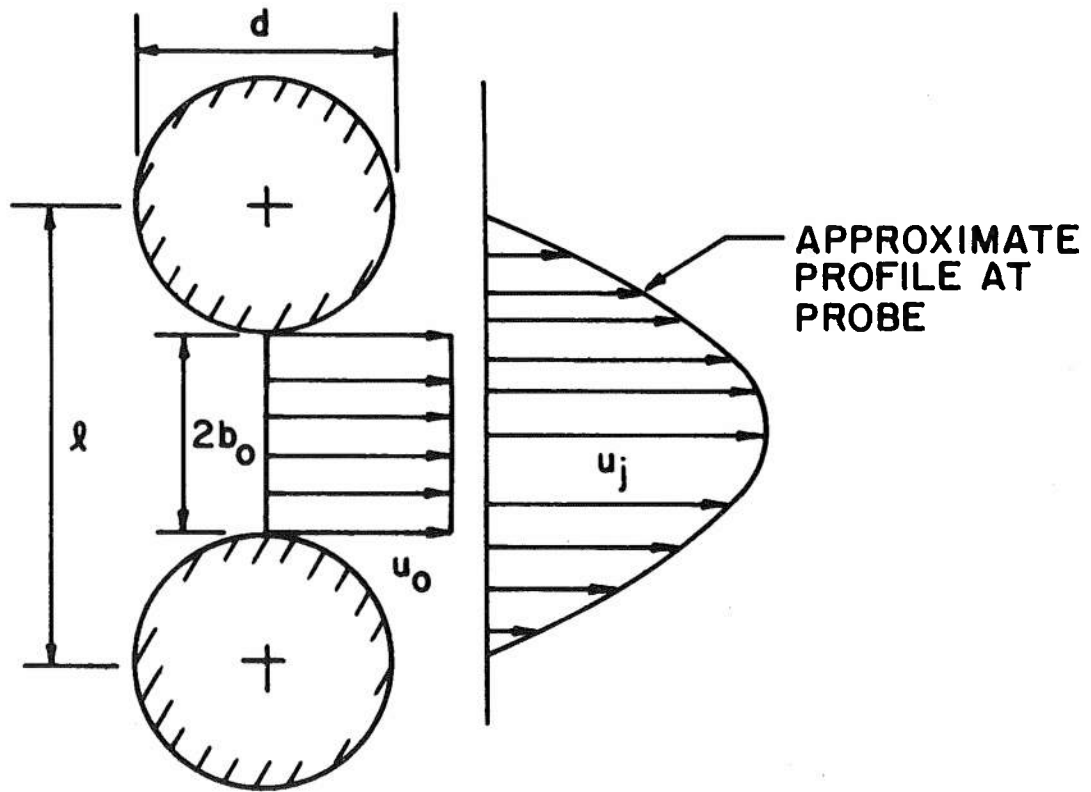


Fig. 11 Relation Between Measured Velocity Profile and Average Velocity Between Adjacent Tubes

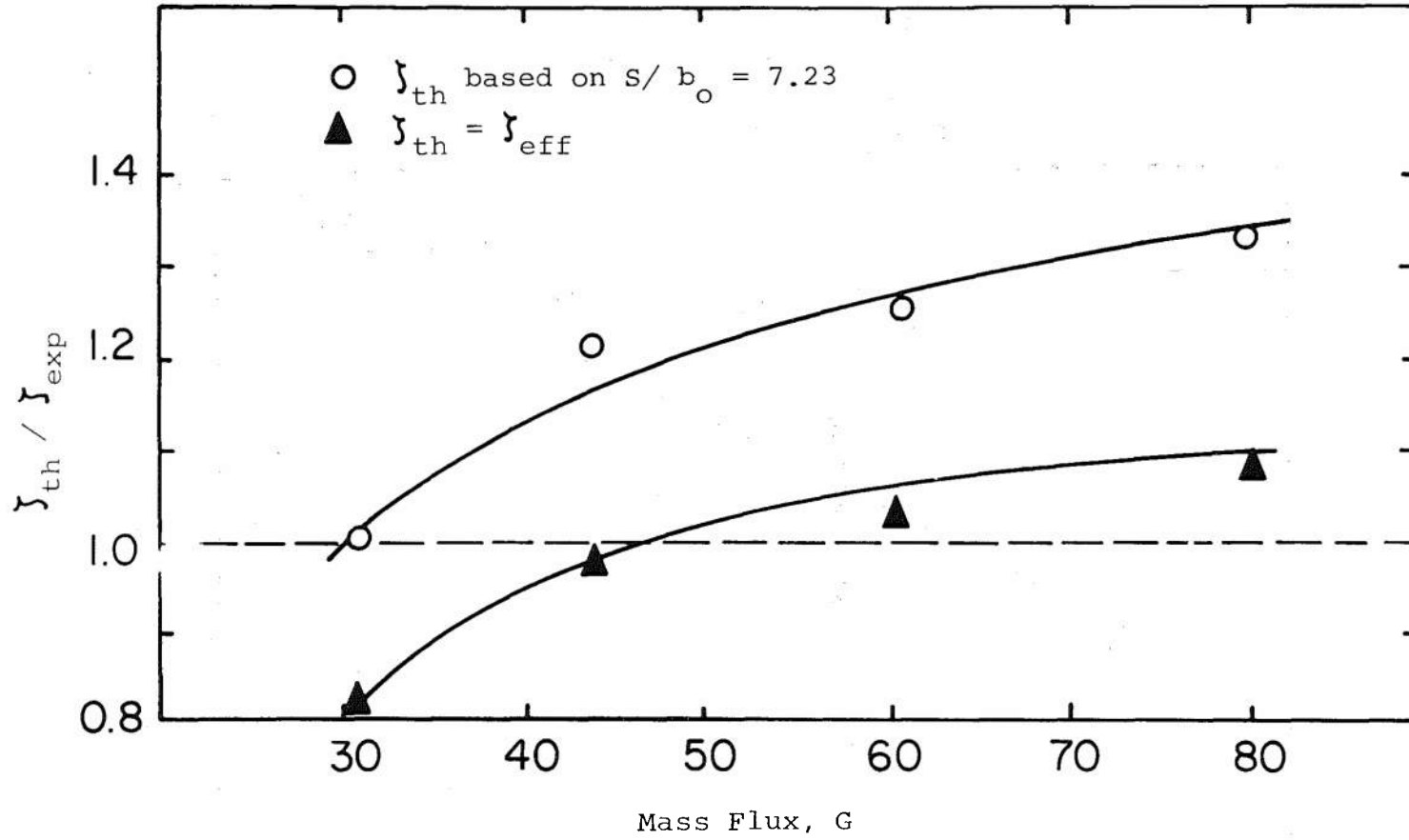


Fig.12 Ratio of Theoretical to Experimental Values of Pressure Loss Coefficient as a Function of Mass Flux

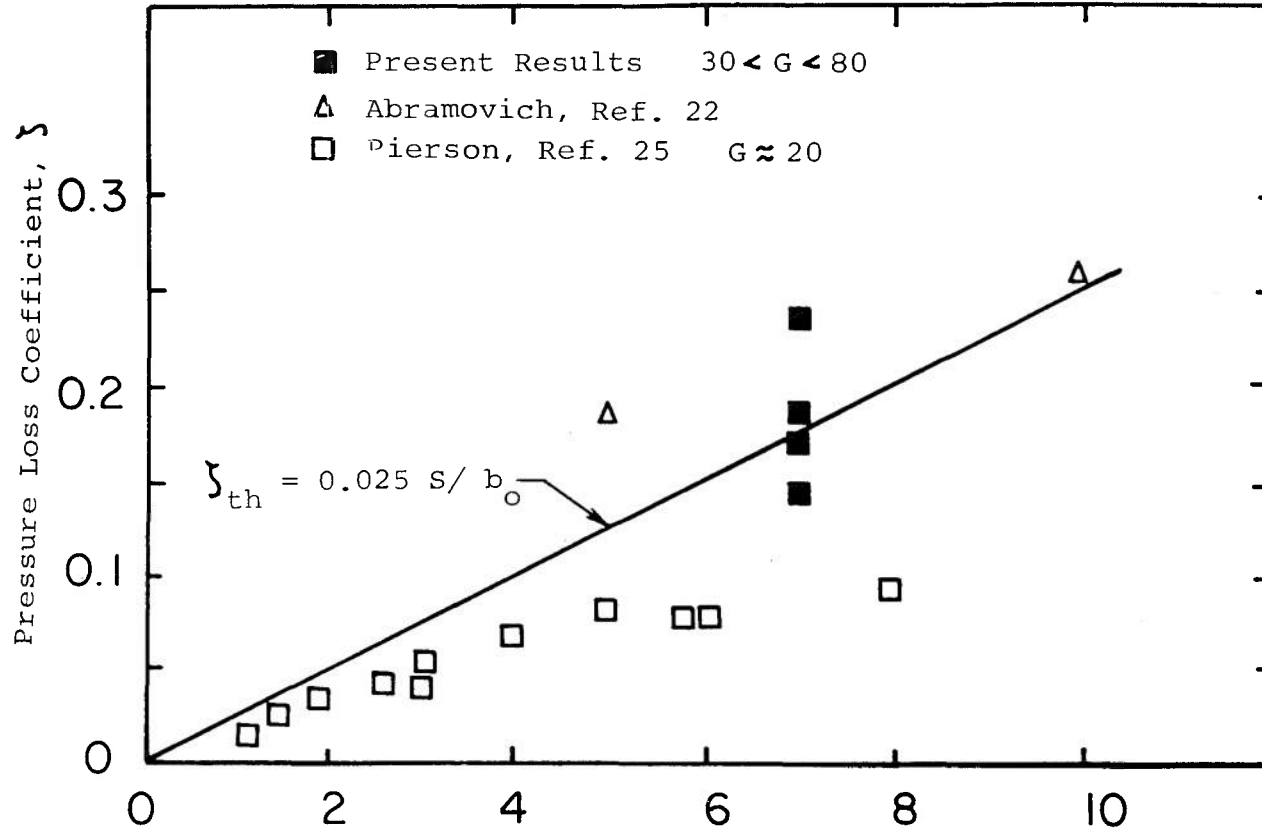
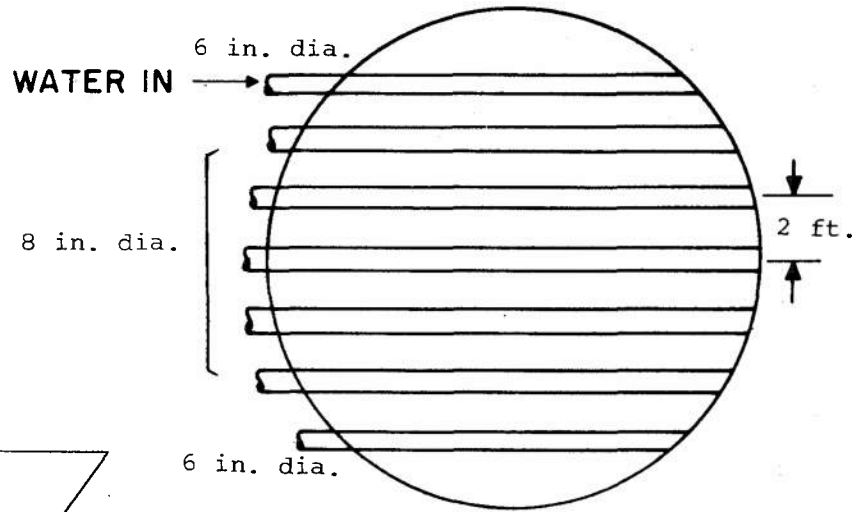


Fig. 13 Comparison of Present Theory and Experimental Data With Results of Other Investigations of In-line Tube Banks

$S = 5.166 \text{ ft.}$   
 $b_o = 0.667 \text{ ft.}$   
 $L = 2.0 \text{ ft.}$



SPRAY BAR  
 LOCATIONS (EIGHT  
 TOTAL)

6 in. dia.

Bar Spacing 5 ft. 2 in.

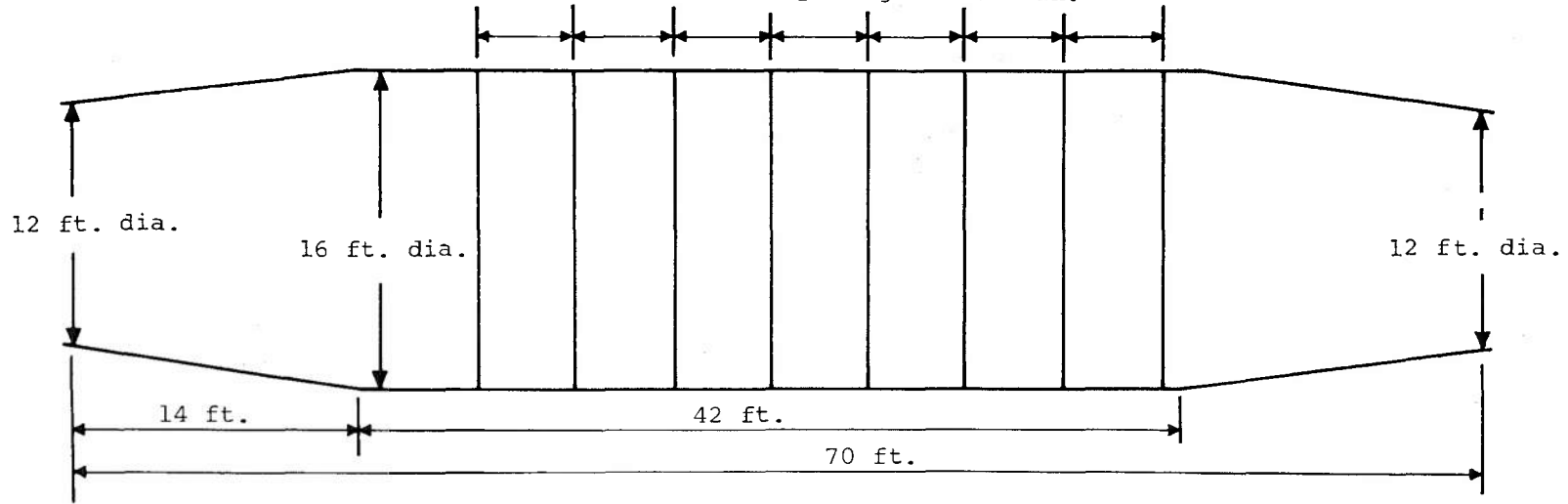
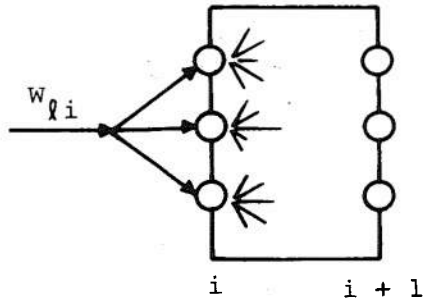
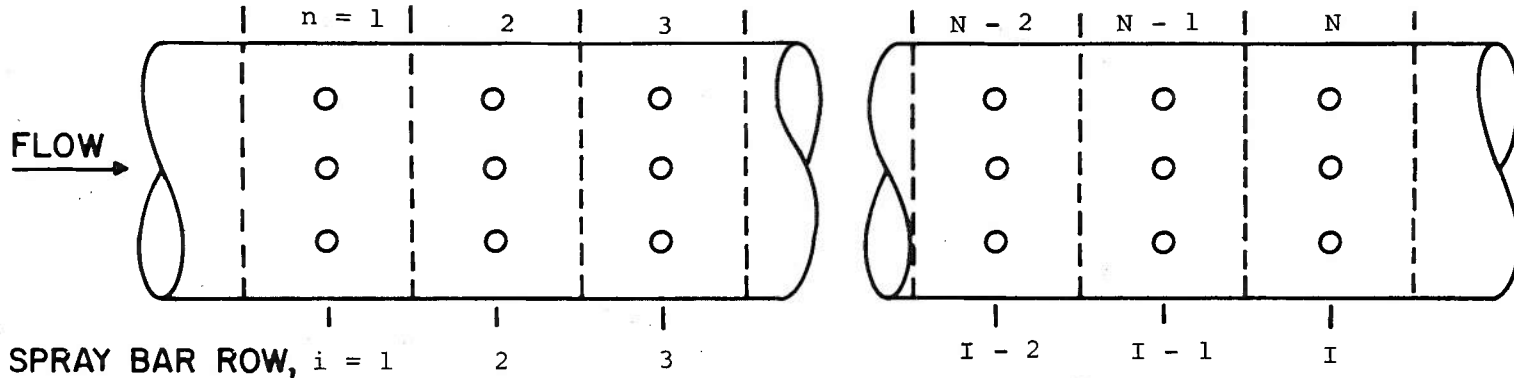
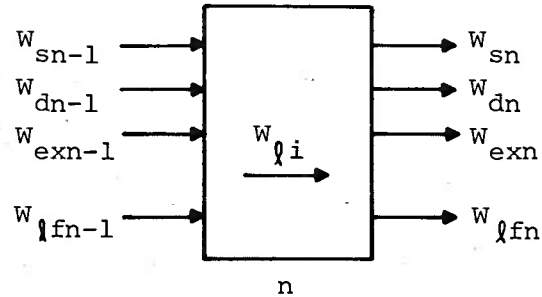


Fig. 14 Spray Cooler Configuration for J-5 Rocket Test Facility

CONTROL VOLUME,



Control Volume for Tube Drag Losses



Control Volume for Other Momentum Losses

Fig. 15 Control Volumes for Spray Cooler Analysis

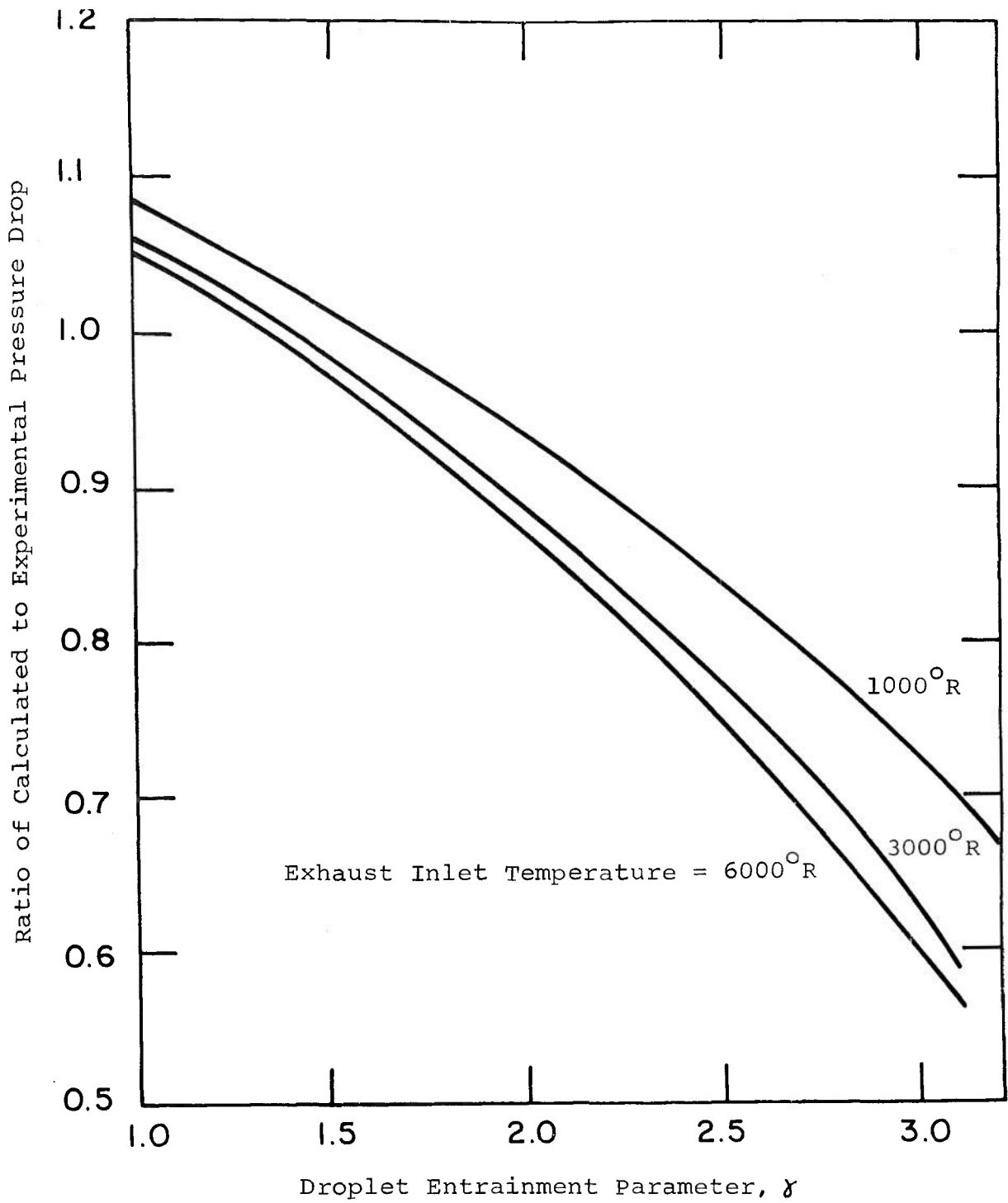


Fig. 16 Pressure Drop Ratia Versus Entrainment Parameter Parametric in Exhaust Inlet Temperature: Data Line 4

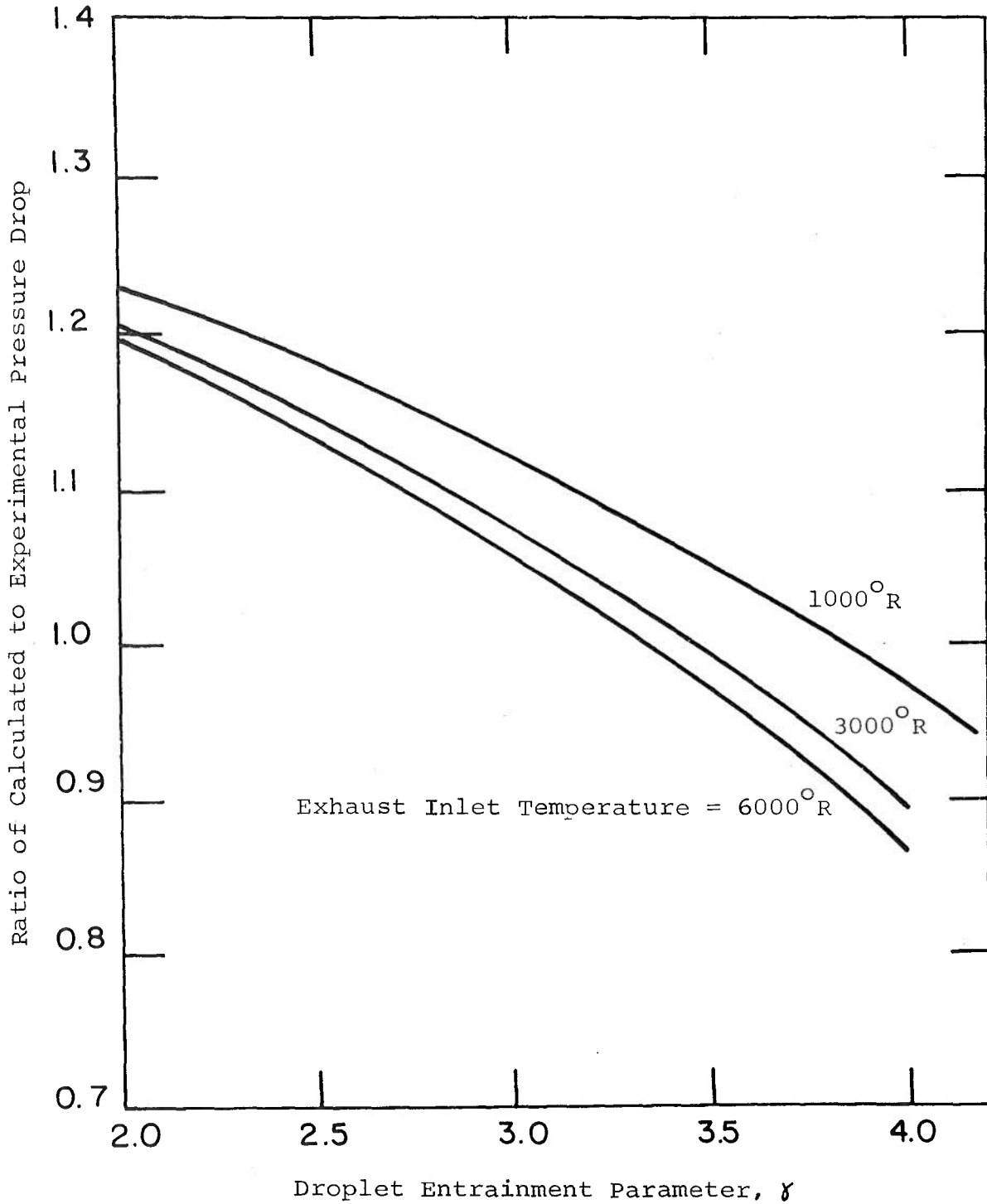


Fig. 17 Pressure Drop Ratio Versus Entrainment Parameter Parametric in Exhaust Inlet Temperature: Data Line 5

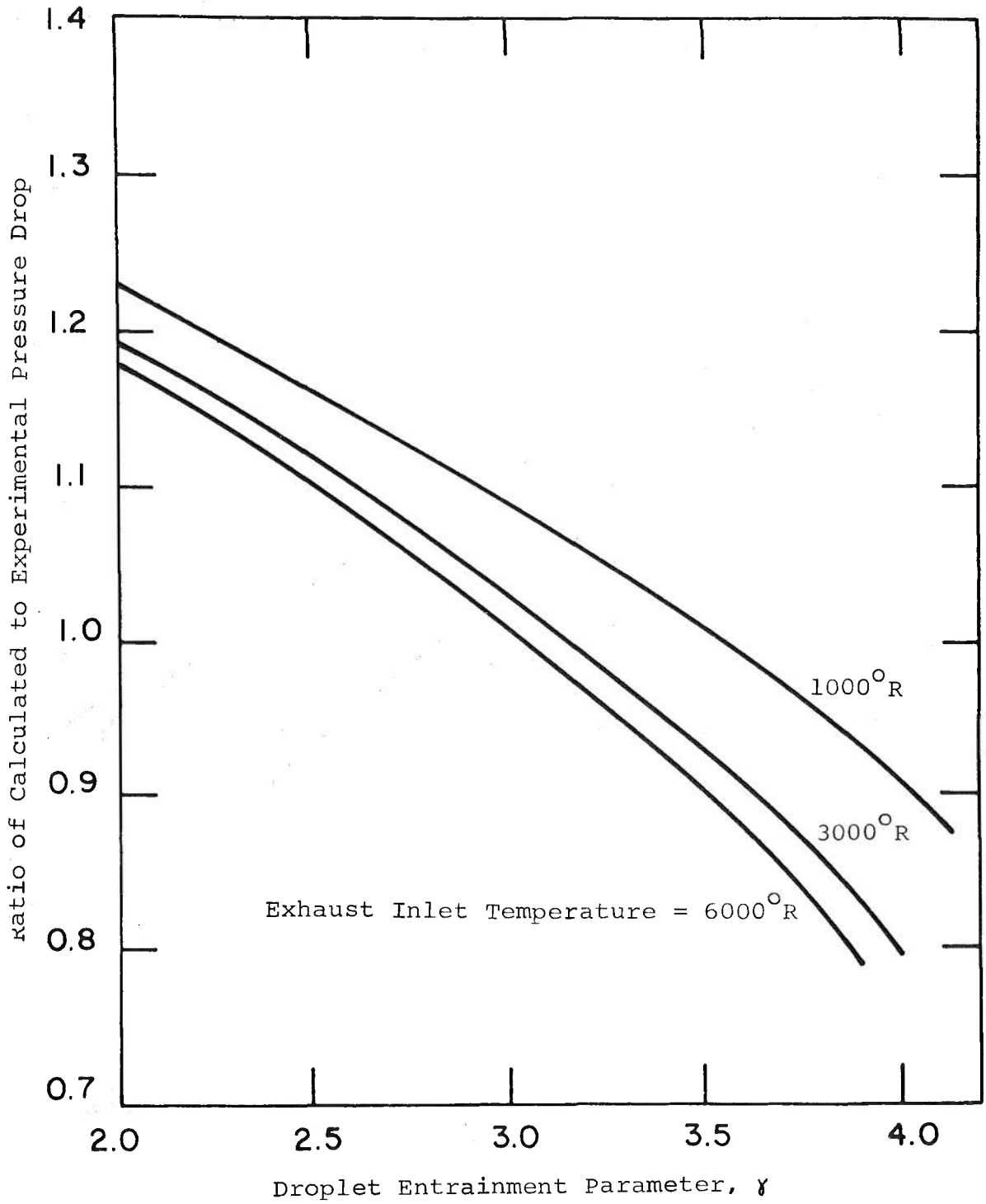


Fig. 18 Pressure Drop Ratio Versus Entrainment Parameter Parametric in Exhaust Inlet Temperature: Data Line 6

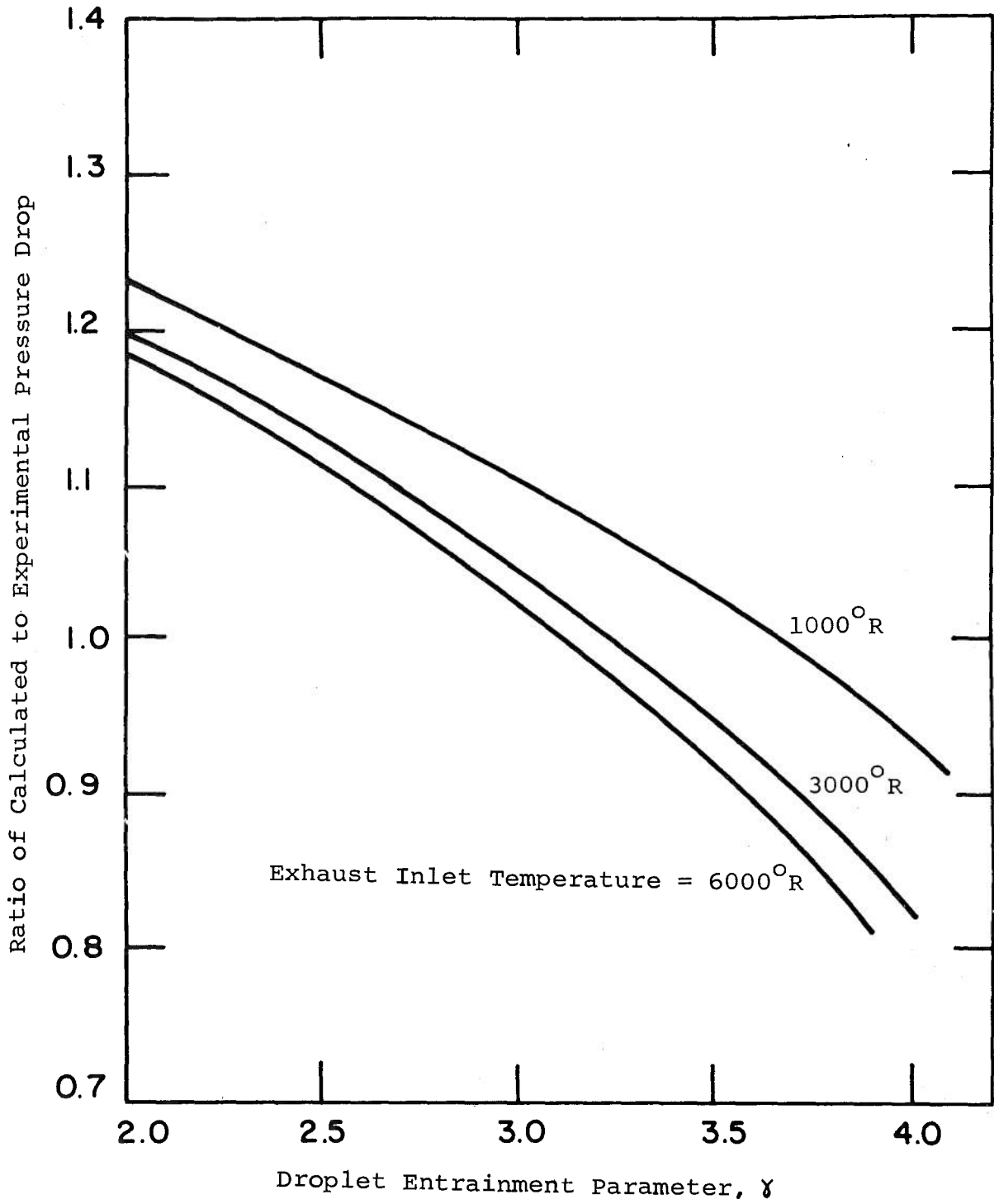


Fig. 19 Pressure Drop Ratio Versus Entrainment Parameter Parametric in Exhaust Inlet Temperature: Data Line 8

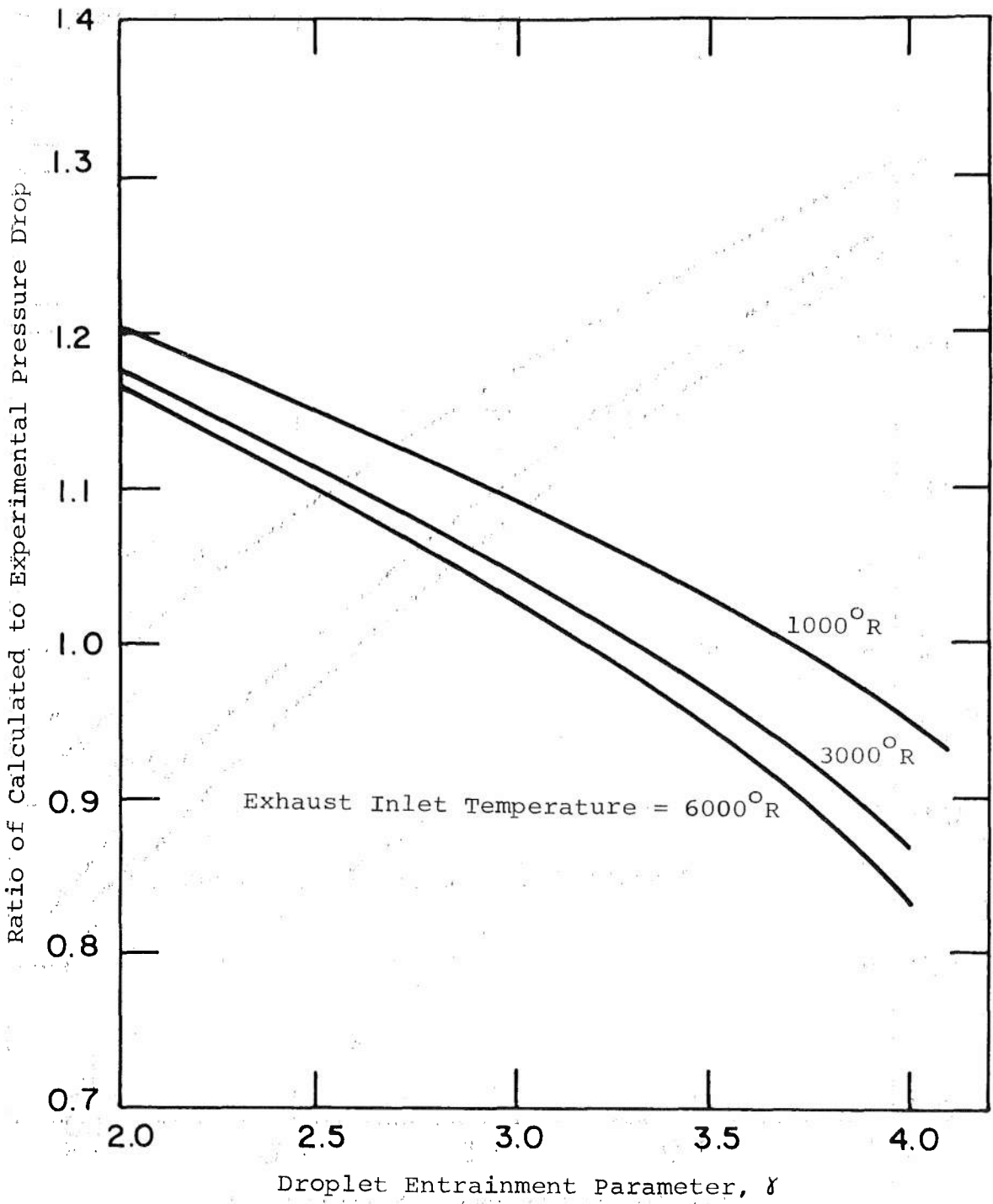


Fig. 20 Pressure Drop Ratio Versus Entrainment Parameter Parametric in Exhaust  
 Inlet Temperature: Data Line 9

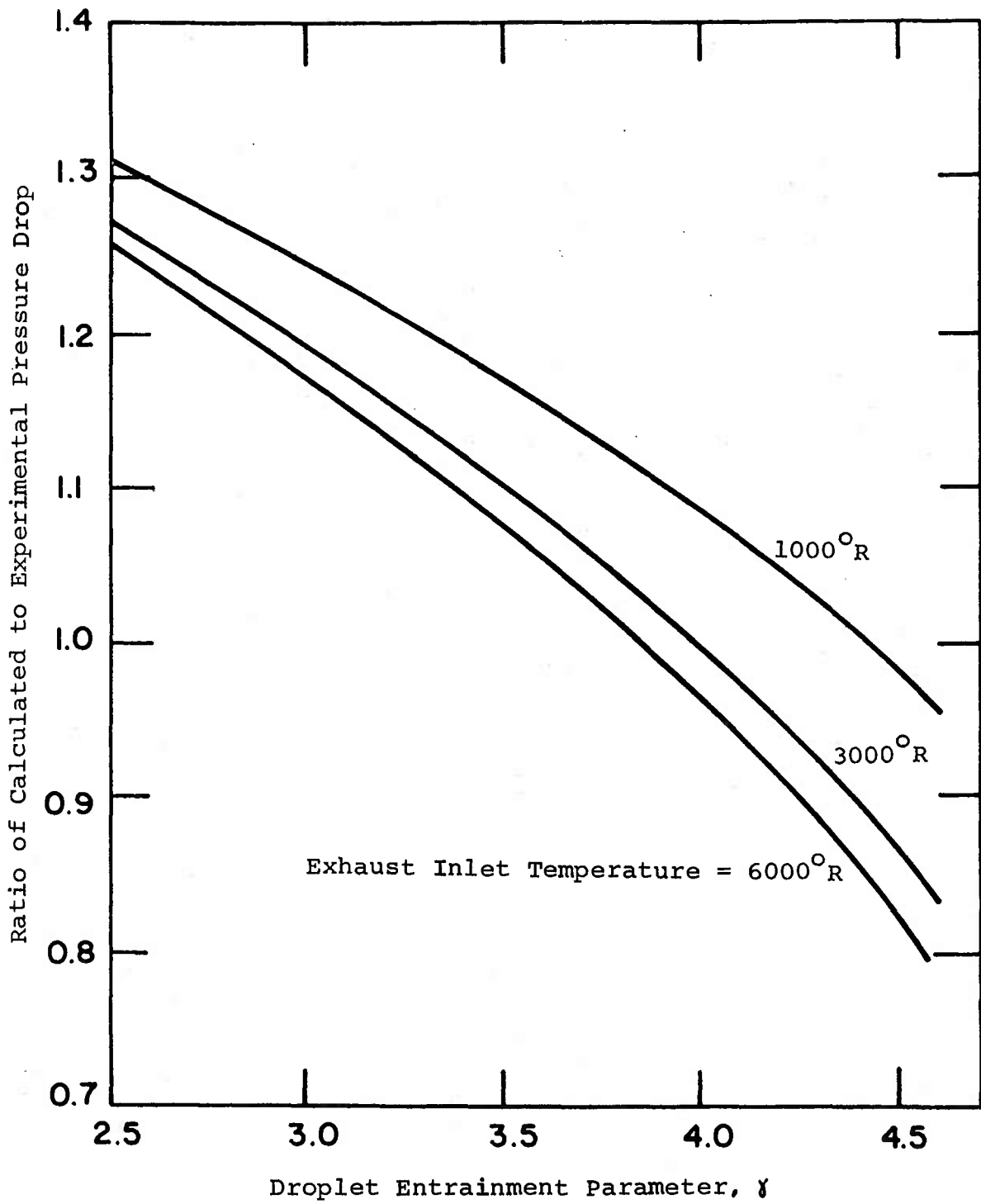


Fig. 21 Pressure Drop Ratio Versus Entrainment Parameter Parametric in Exhaust Inlet Temperature: Data Line 10

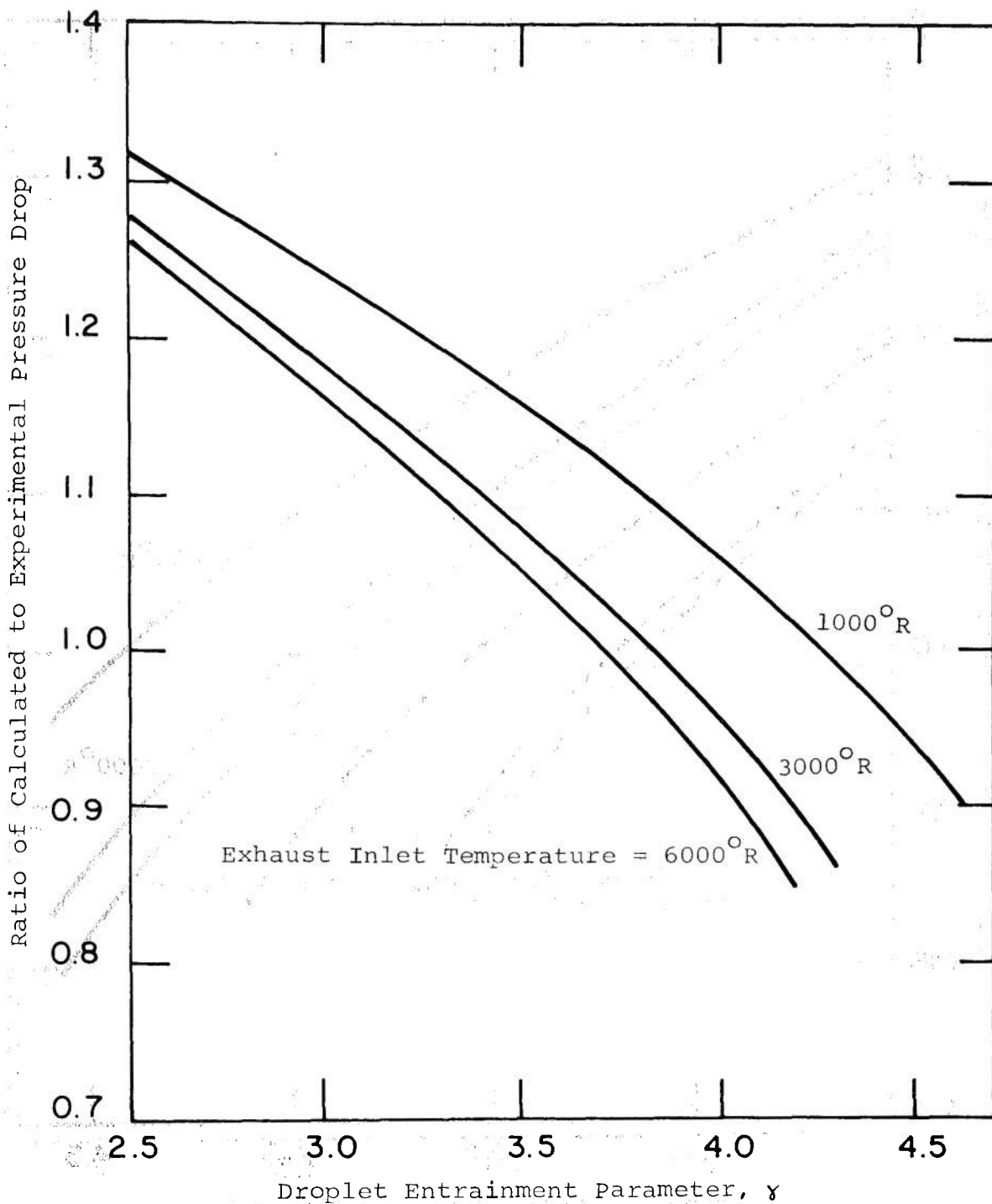


Fig. 22 Pressure Drop Ratio Versus Entrainment Parameter Parametric in Exhaust Inlet Temperature: Data Line 11

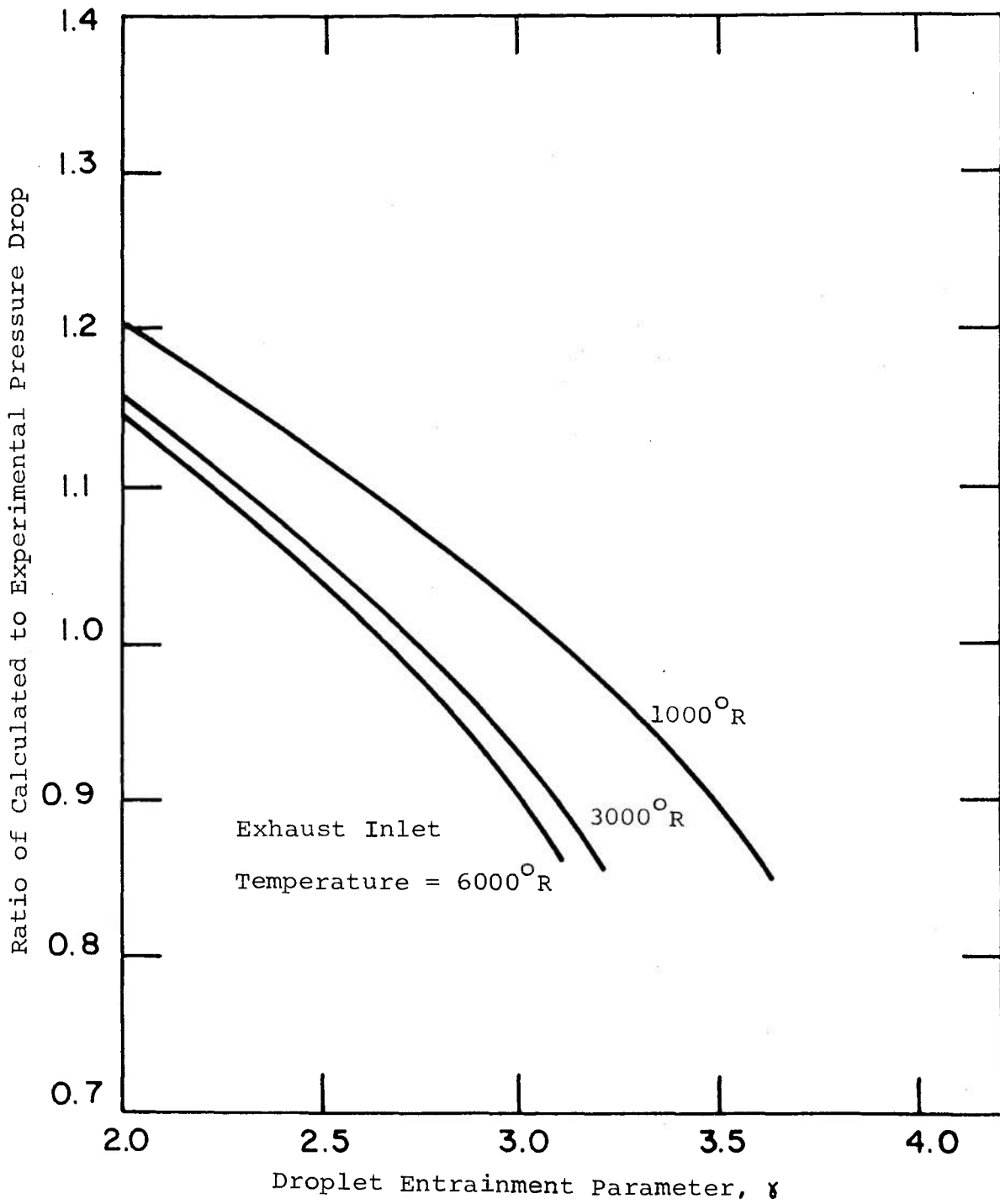


Fig. 23 Pressure Drop Ratio Versus Entrainment Parameter Parametric in Exhaust Inlet Temperature: Data Line 12

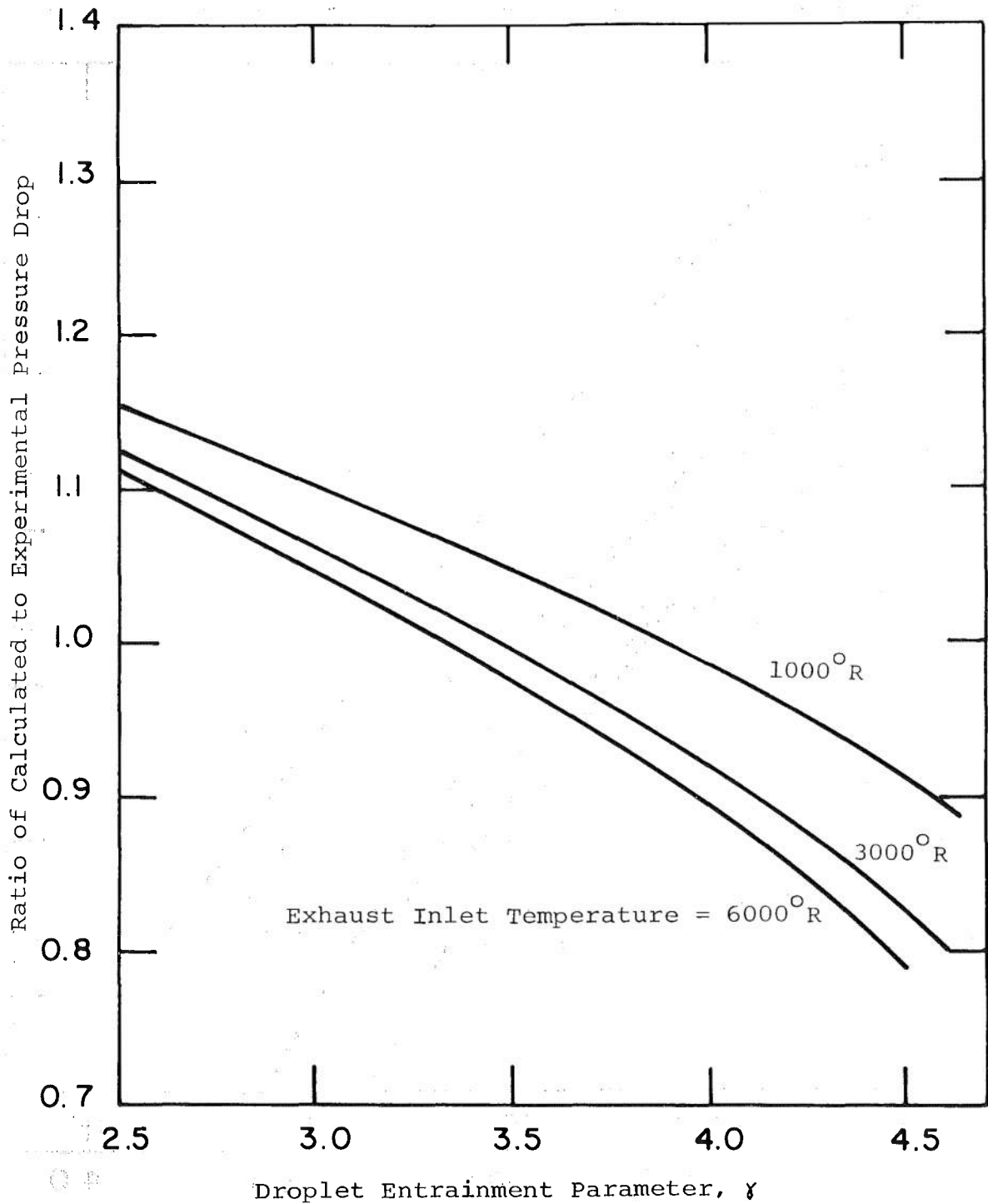


Fig. 24 Pressure Drop Ratio Versus Entrainment Parameter Parametric in Exhaust Inlet Temperature: Data Line 13

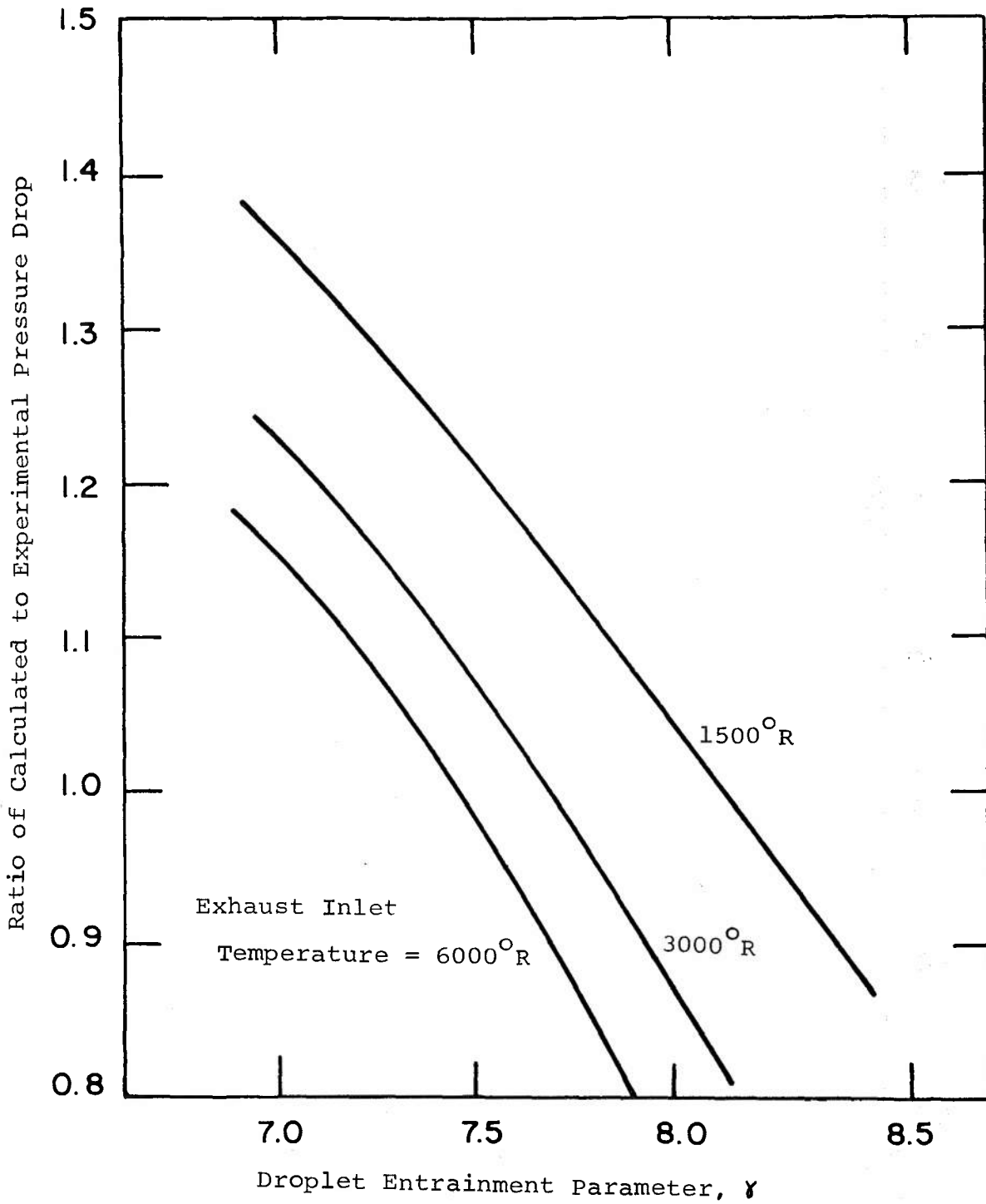


Fig. 25 Pressure Drop Ratio Versus Entrainment Parameter Parametric in Exhaust Inlet Temperature: Data Line 14

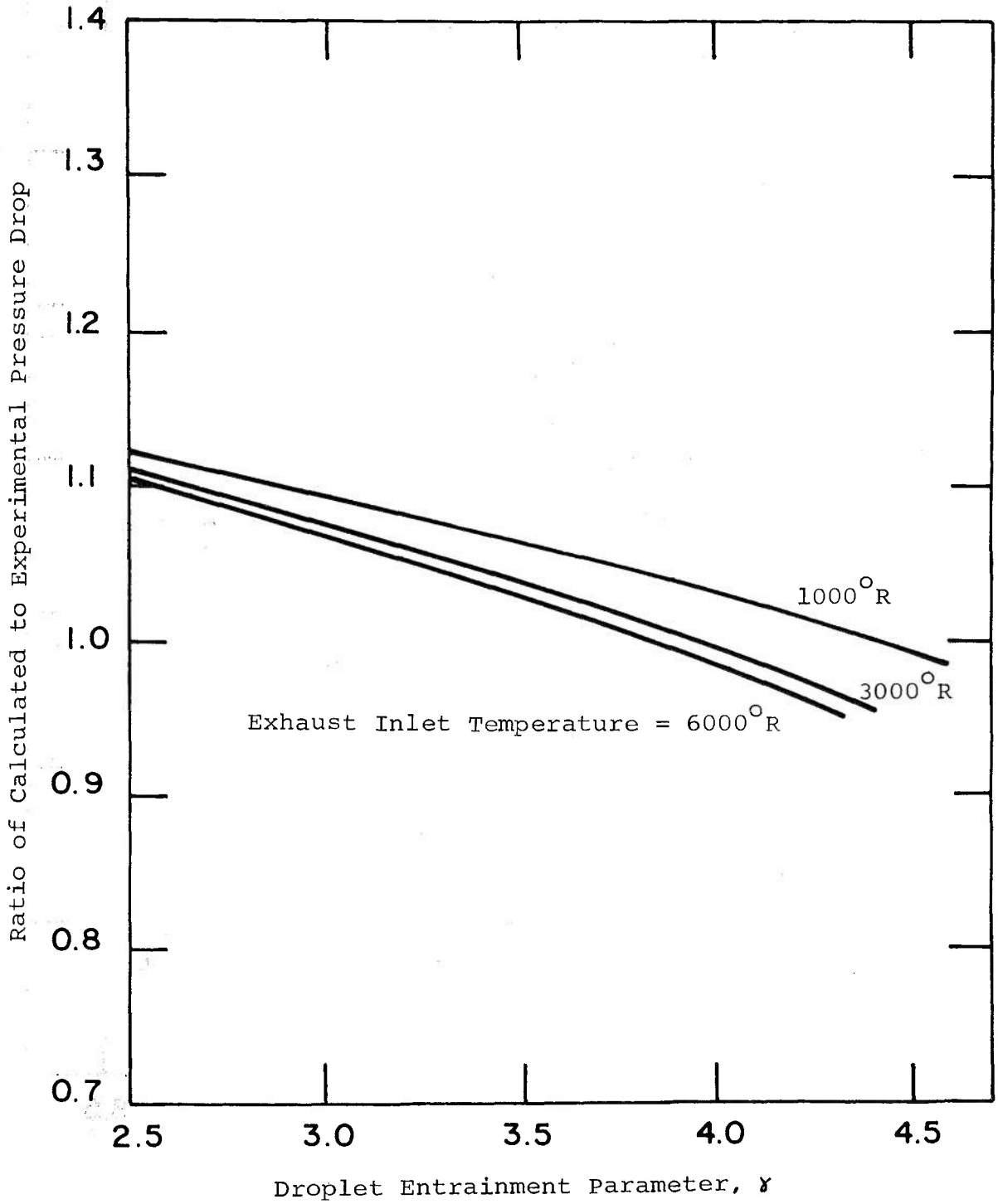


Fig. 26 Pressure Drop Ratio Versus Entrainment Parameter Parametric In Exhaust Inlet Temperature: Data Line 15

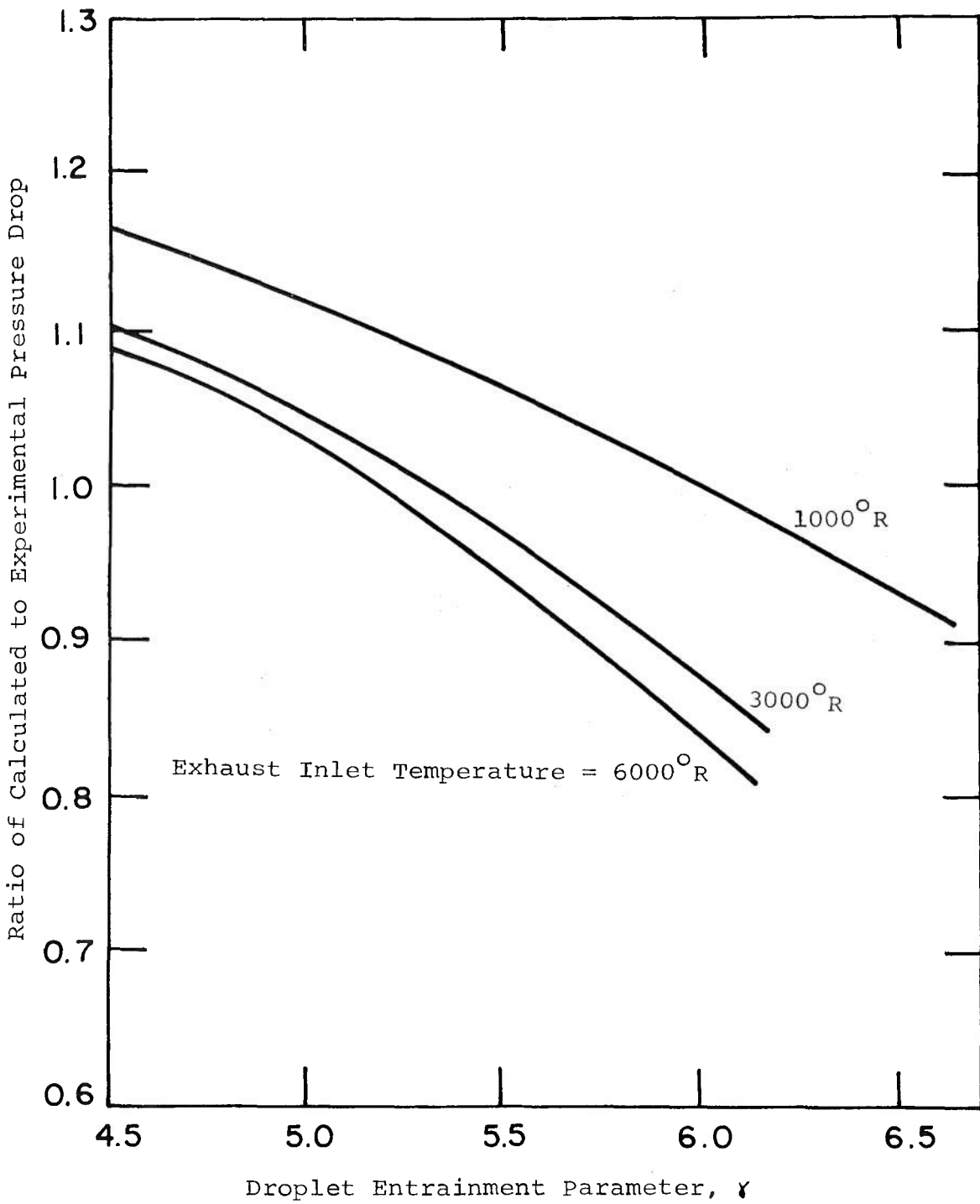


Fig. 27 Pressure Drop Ratio Versus Entrainment Parameter Parametric in Exhaust Inlet Temperature: Data Line 16

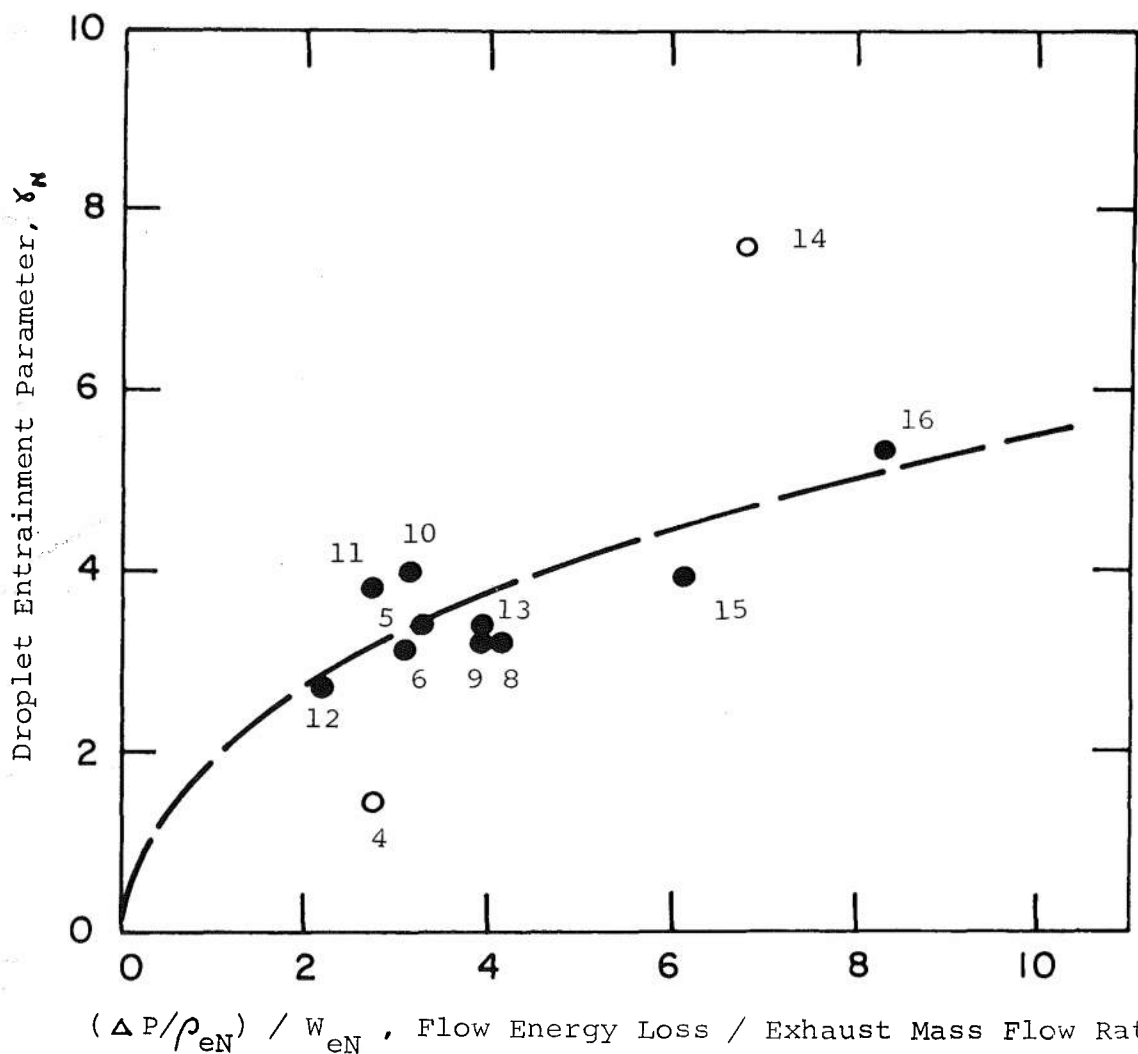


Fig. 28 Correlation of Droplet Entrainment Parameter with Ratio of Flow Energy Loss to Exhaust Outlet Mass Flow Rate

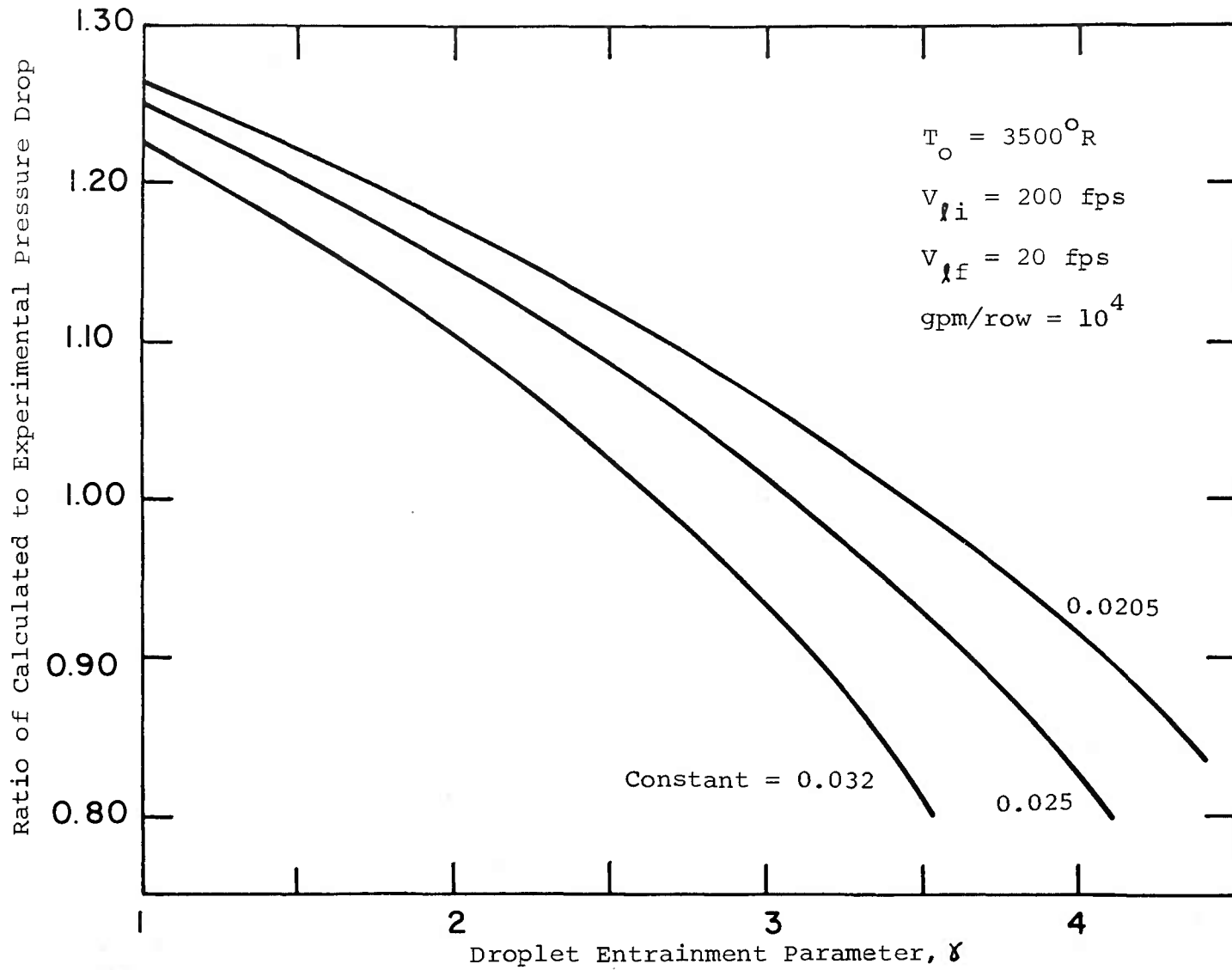


Fig. 29 Effect of Pressure-Loss-Coefficient Constant on Pressure Drop Ratio as a Function of Entrainment Parameter: Data Line 13

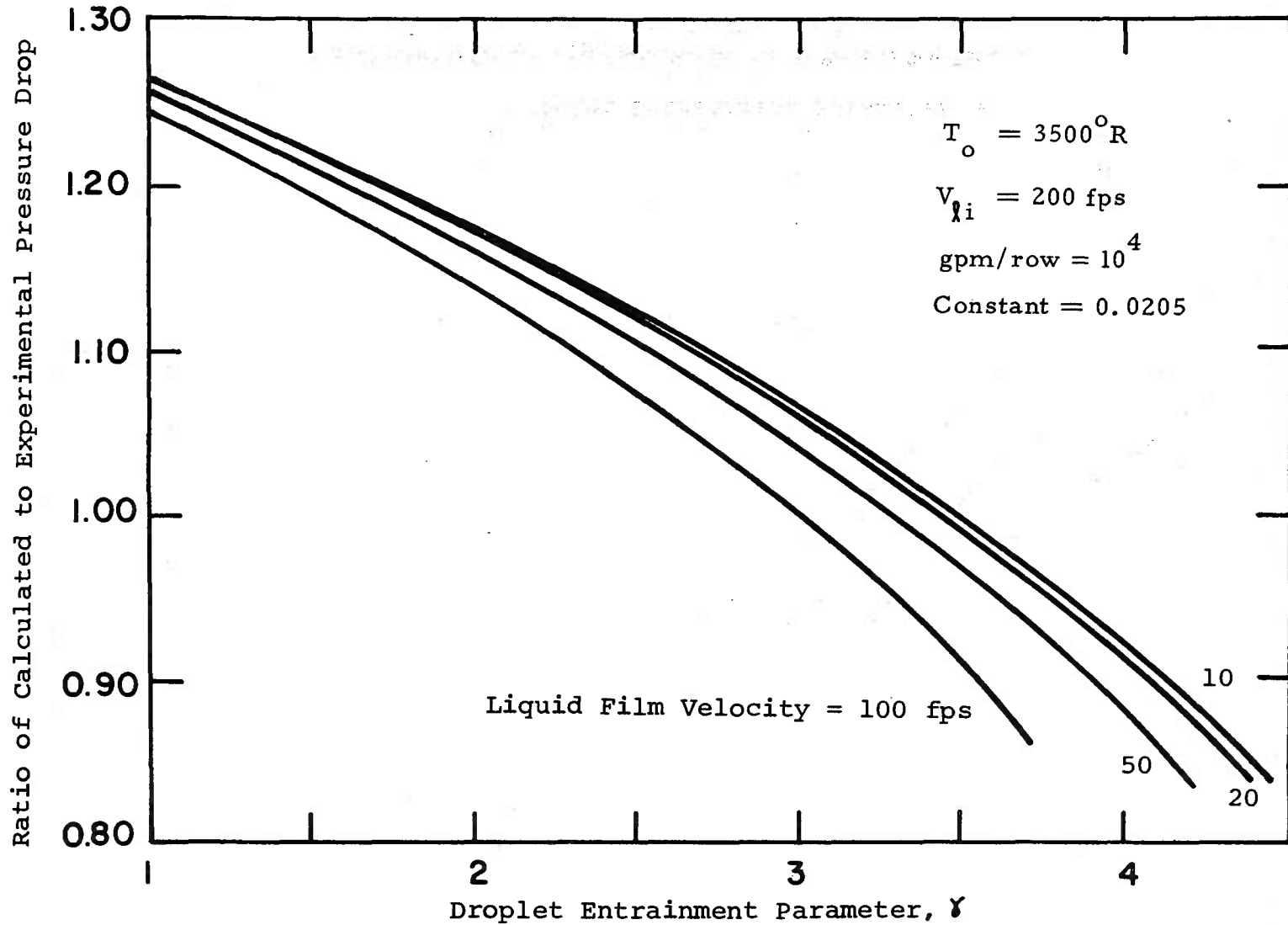


Fig. 30 Effect of Liquid Film Velocity on Pressure Drop Ratio as a Function of Entrainment Parameter: Data Line 13

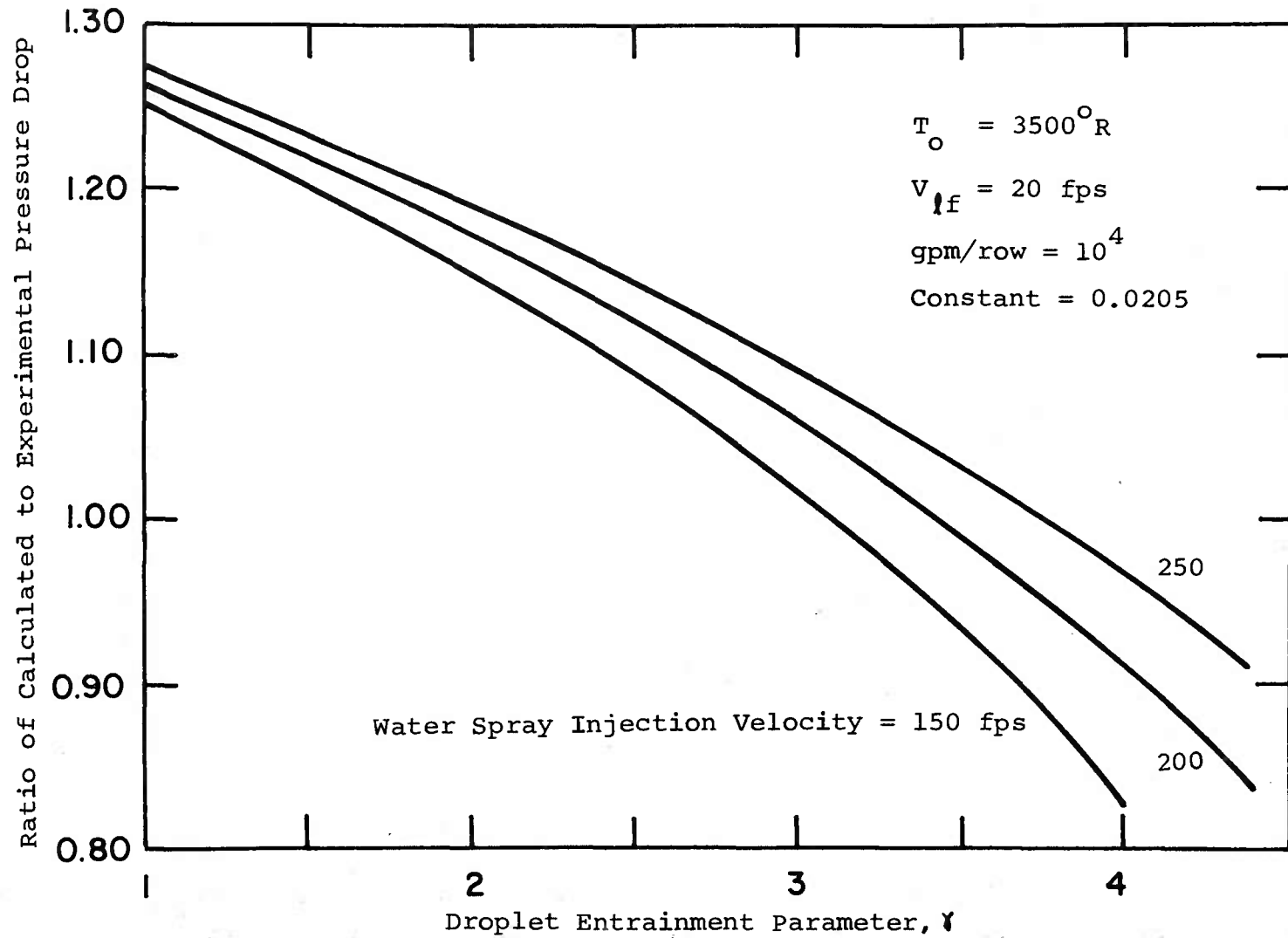


Fig. 31 Effect of Water Spray Injection Velocity on Pressure Drop Ratio as a Function of Entrainment Parameter: Data Line 13

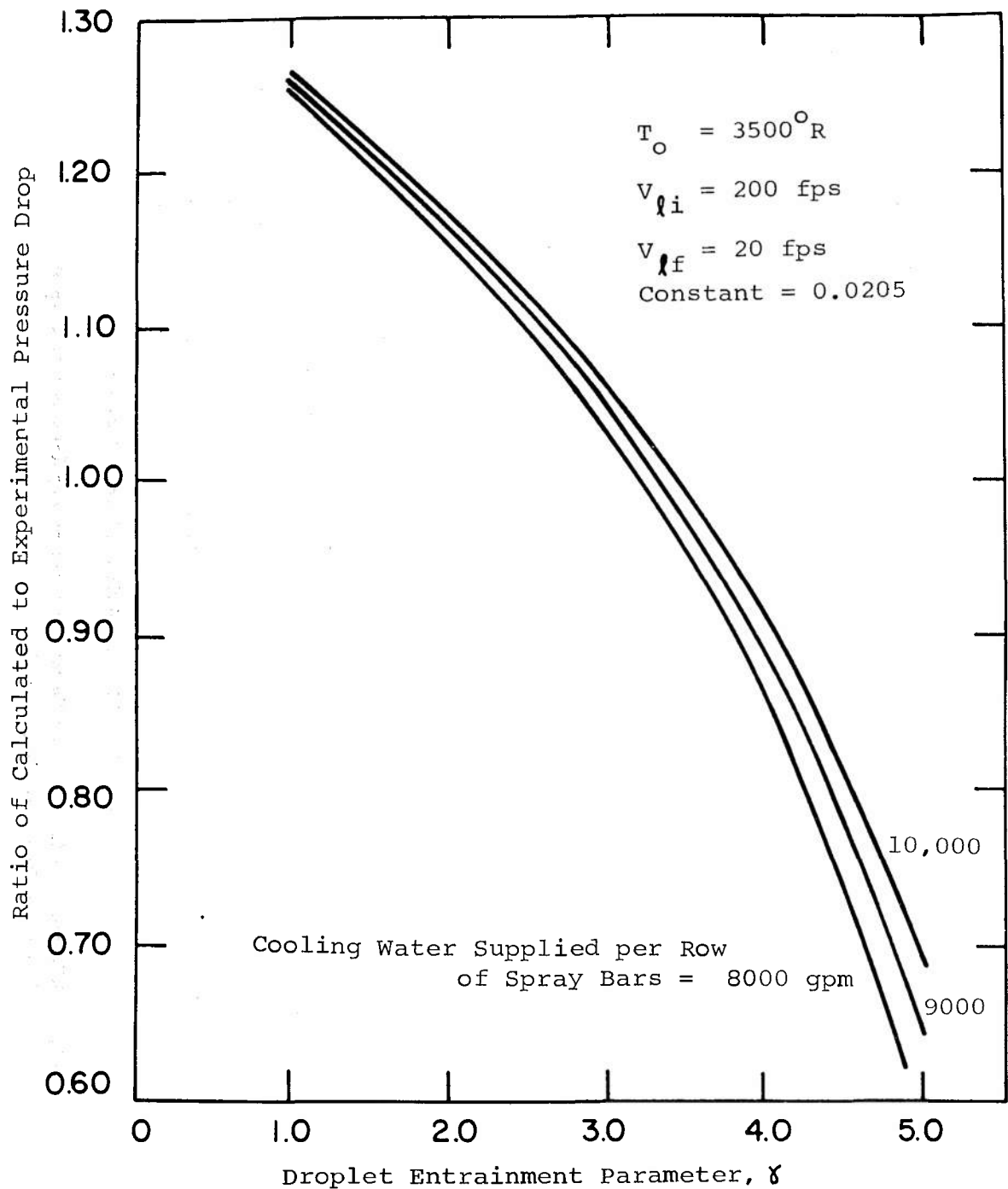


Fig. 32 Effect of Cooling Water Flow Rate Supplied per Row of Spray Bars  
 on Pressure Drop Ratio as a Function of Entrainment Parameter:  
 Data Line 13

UNCLASSIFIED

Security Classification

## DOCUMENT CONTROL DATA - R &amp; D

*(Security classification of title, body of abstract and indexing annotation must be entered when the overall report is classified)*

1. ORIGINATING ACTIVITY <i>(Corporate author)</i> University of Texas at Austin College of Engineering, Austin, Texas 78712		2a. REPORT SECURITY CLASSIFICATION UNCLASSIFIED	
		2b. GROUP N/A	
3. REPORT TITLE TWO-PHASE FLOW IN SPRAY COOLERS			
4. DESCRIPTIVE NOTES <i>(Type of report and inclusive dates)</i> Final Report, April 1966 - August 1967.			
5. AUTHOR(S) <i>(First name, middle initial, last name)</i> H. A. Walls, J. P. Lamb, et al.			
6. REPORT DATE June 1968	7a. TOTAL NO. OF PAGES 89	7b. NO. OF REFS 26	
8a. CONTRACT OR GRANT NO. AF 40(600)-1167	9a. ORIGINATOR'S REPORT NUMBER(S) AEDC-TR-68-127		
b. PROJECT NO. 5730	9b. OTHER REPORT NO(S) <i>(Any other numbers that may be assigned this report)</i> N/A		
c. Program Element 6240518F			
d. Task 573004			
10. DISTRIBUTION STATEMENT This document has been approved for public release and sale; its distribution is unlimited.			
11. SUPPLEMENTARY NOTES  Available in DDC.		12. SPONSORING MILITARY ACTIVITY Arnold Engineering Development Center, Air Force Systems Command, Arnold AF Station, Tenn. 37389	
13. ABSTRACT The problem of estimating pressure drops with typical in-line bar, spray cooler configurations is discussed. Such coolers form an important component of facilities for rocket testing at simulated altitudes. In the present report, the complex nature of gas-liquid flows is first discussed. This is followed by a presentation of results of some simple experiments of air flow over a tube bank in a model spray-cooler section to determine the influence of this particular geometry on the drag coefficient. Based upon the information in these two sections, a semi-empirical analysis of two-phase flow in coolers is then developed and some results of the method are presented. Finally, recommendations are made concerning an experimental program which would enhance the further development of prediction techniques in cooler design.			

14. KEY WORDS	LINK A		LINK B		LINK C	
	ROLE	WT	ROLE	WT	ROLE	WT
spray coolers exhaust gas cooling two-phase gas flow droplet entrainment parameter						